Technical Report 1679
September 1994

Interactions of a Target with its Acoustic Environment

E. P. McDaid
D. Gillette
D. Barach

Technical Report 1679
September 1994

Interactions of a Target with its Acoustic Environment

E. P. McDaid
D. Gillette
D. Barach

EXECUTIVE SUMMARY

OBJECTIVES

The objective of this project was to find a solution to the hollow core cable breakage problem in the VLF Cutler topload. A field survey was conducted. Some candidate solutions were developed and costed out. Drawings and specifications were prepared for two of these options.

RESULTS

The findings of the field survey were the following: (l) The 225-ft sections of hollow core have never been observed to break; only the 775-ft sections have broken. (2) Severe icing conditions often exist at Cutler during winter, and deicing is necessary for the topload conductors. The support catenary does not deice, and short sections of conductor cable could be attached to it that would not deice. (3) No spare Calsun bronze® or hollow core cable was on site. The spare cable on site is not suitable as a topload conductor because it does not have enough resistance to deice properly. (4) The panel hoist winches are already at maximum load, and increasing the total weight in the topload panels is not practical.

Maintaining the existing operational capability to operate at full power down to 14 kHz is desirable in order to provide contingency long-range coverage when using the planned split-array mode. One operational area that could be reached in this way is the Arabian Sea. Surface electric field calculations indicate that a 1.5-inch-diameter cable is necessary to eliminate corona formation at the lower frequencies. This eliminates the option of repairing the hollow core cable by replacing the end fittings and making up the lost length by extension of the l-inch-diameter Calsun bronze.

CONCLUSIONS

Four options are presented that retain full existing operational capability, and replace or repair only the 775-ft hollow core sections. Option 2 is the recommended long-term solution with option 4 recommended for short-term, or emergency repairs if necessary. Options 1 and 3 are included as contingencies.

(1) Replace the 775-ft sections of hollow core with a specially made 1.47-inch-diameter cable having a stainless steel core and copper alloy exterior. This will add 7750 lbs to the outer portion of the topload and requires a commensurate reduction in insulator weight. The amount of weight reduction required cannot be achieved by removing insulators from the existing strings of Lapp insulators without reducing the withstand voltage below acceptable limits. Thus, this option requires replacing the Lapp insulators with new Racal-Decca safety core insulators. The cost of this option is $2.2M for the new cables installed, with another $0.75M for the new insulators.

(2) Cut and replace the end fittings on the hollow core, retaining a 250-ft section while replacing the remaining 550 ft with a specially made 1.3-inch-diameter cable having a stainless steel core and copper alloy exterior. The cost of the cable alone for this option is estimated to

be $1.43M ($0.75M less than option 1). This option adds less weight to the topload so compensating weight reduction can be accomplished by removal of a few Lapp insulators; thus, saving the cost of new insulators (an additional $0.75M). The only drawback is the lack of experience in the manufacture of composite cables and some uncertainty as to the breaking strength of this cable. This is not a serious drawback as the breaking strength will likely be acceptable for the Cutler application.

(3) Cut and replace the end fittings on the hollow core sections, while retaining as much cable as possible. The total length cut out by this and the previous repair would be approximately 16 ft, which would be made up with 1.5-inch copperweld cable (nondeicing) located at the support catenary end. This solution is less expensive (estimated at $500k) and extends the hollow core life about 10 years, at which time the same repair could be repeated by using a longer (25-ft) section of copperweld.

(4) Repair the existing hollow core by cutting and replacing the end fittings only on severely damaged sections. Replace the missing 16 ft of hollow core with 1.01-inch copperweld having a 1-inch copper jumper in parallel (nondeicing) as a 2-wire cage with cable separation of 4 inches, center to center. VLF Jim Creek has copperweld cable available and can produce the sections. The major cost is installation, which could be done by Cutler personnel.

Drawings have been prepared by LANTNAVFACENGCOM for options 3 and 4, which are included as appendix E. Originally, option 3 was to be the interim or emergency fix. However, option 4, which was developed after preparation of the option 3 drawings, is the simplest and least expensive and, therefore, became the recommended option for interim or emergency repairs.

RECOMMENDATIONS

(l) The above options range from a permanent, but expensive, 100% replacement program to an inexpensive interim repair for individual cables as needed. Since the extent of the problem cannot be known until the internal condition of the cables is determined, it is recommended that the Navy x-ray all 192 hollow core connections before deciding which option to pursue.

(2) Jim Creek personnel should prepare some 1.01-inch-diameter copperweld sections according to the drawings provided and ship them to Cutler to have available as an interim or emergency fix (option 4) should the x-ray program indicate that any hollow core cables have six or more broken wires. Also, procure the special clamps required to maintain the 4-inch center-to-center spacing between the copperweld cable and the 1-inch copper jumper.

(3) A firm price should be obtained from vendors for the recommended 1.3-inch-diameter cables, and plans and costs developed for the installation of option 2 as the permanent fix.

(4) No spare cable exists on site for either the l-inch-diameter Calsun bronze or the 1.5-inch hollow core conductor cables used in the Cutler antenna topload. No vendor can supply either of these cables off-the-shelf. We did, however, find an off-the-shelf alumoweld cable, 1.01 inches in diameter, that could be used as a direct replacement for the Calsun bronze. If the alumoweld cable is installed as a partial replacement, and is in contact with copper alloy cables, suitable bimetallic fittings will be needed to reduce electrolytic corrosion.

CONTENTS

INTRODUCTION 1

MULTIPLE SCATTERING 2

APPARENT TARGET STRENGTH 5

INTERMODAL SCATTERING STRENGTH 6

CALCULATED RESULTS 8

CONCLUSIONS 9

REFERENCES 15

APPENDIX A-1

FIGURES

1. Source/target/receiver arrangement for shallow duct 10
2. Apparent target strength of hard sphere in uniform duct with hard bottom 11
3. Apparent target strength of hard sphere in convergence zone 11
4. Apparent target strength of rigid cylinder in duct. End aspect 12
5. Multiple scattering effects on apparent target strength of rigid sphere near surface. Target depth /a = 7 12
6. Multiple scattering effects on apparent target strength of rigid sphere near surface. Target depth /a = 2 13
7. Multiple scattering effects on apparent target strength for rigid sphere near rigid bottom. Target depth /a = 53 13
8. Multiple scattering effects on apparent target strength for rigid sphere near hard bottom. Target depth /a = 58 14
9. Effect of Fresnel terms on apparent target strength for rigid cylinder with end caps. Target at center of duct and at beam aspect 14

INTRODUCTION

An approach to the problem of calculating the pressure field scattered by a structure immersed in a nonuniform fluid environment has been reported in McDaid et al. (1992). The method is based on the Helmholtz integral equation formulation of fluid loading in a stratified medium and on a finite element formulation of the dynamics of the structure.

A set of Helmholtz Integral Equations has been derived which have as kernels the Green's function (and its gradient) for a refractive environment with boundaries. The relevant equations are reproduced below. A detailed derivation of the equations has been relegated to the appendix to preserve the continuity of the main body of the report.

First, there is the Surface Integral Equation relating the distribution of pressures and velocities on the wetted surface of the target, which have been induced by the incident (ensonifying) pressure generated by a distant point source of sound:

$$\begin{array}{c} \text{surface} \\ \text{pressure} \end{array} \overbrace{P(\vec{R}_{sg}|\vec{R}_{sp})} = \begin{array}{c} \text{incident} \\ \text{pressure} \end{array} \overbrace{G(\vec{R}_{sp}|\vec{R}_{sg})} + \frac{1}{2}$$

$$\int_{S_{sh}} [\underbrace{P(\vec{R}_{sh}|\vec{R}_{sp})}_{\begin{array}{c}\text{surface}\\ \text{pressure}\end{array}} \nabla_{R_{sh}} \underbrace{G_S(\vec{R}_{sh}|\vec{R}_{sg})}_{\begin{array}{c}\text{surface}\\ \text{Green's fcn}\end{array}} - \underbrace{G_S(\vec{R}_{sh}|\vec{R}_{sg})}_{\begin{array}{c}\text{surface}\\ \text{Green's fcn}\end{array}} \nabla_{R_{sh}} \underbrace{P(\vec{R}_{sh}|\vec{R}_{sp})}_{\begin{array}{c}\text{surface}\\ \text{pressure}\end{array}}] \cdot \vec{n}_{sh} dS \ , \tag{1}$$

where $\vec{R}_{sp}$, and $\vec{R}_{sg}$ are the positions of the locations of the ensonifying source point, the field point on the target at which pressures are to be calculated and an integration point (dummy variable) on the target surface. The quantity $\vec{n}_{sh}$ is the unit outward normal vector to the wetted surface of the target.

The foregoing equation (1) employs an approximation that reduces the computational burden, viz., that the kernel of the integral equation is an approximate propagation Green's function, G_S, rather than the required refractive Green's function G. The reason for using this approximation is that a tractable implementation of an algorithm for a normal mode representation of the Green's function in the near field is currently not available. McDaid et al. (1992) detailed the results of a study in which the free-space Green's function G_O was used for G_S. The justification of the use of the free-field approximation is that the distances separating pairs of points on the surface are small compared to the distances over which significant refractive effects due to a variable sound speed will occur; and the interpoint distances are small in comparison to the distance to the surface and hence to target "image" points. This latter assumption requires that only those configurations be investigated for which the target is not "near" the boundaries of the medium.

MULTIPLE SCATTERING

The most important of the effects that were ignored by McDaid et al. (1992) was multiple scattering. This phenomenon will be strongest when the target is very near one of the boundaries of the fluid. In the present study, a Neumann series representation of the Green's functions appearing in the Surface Integral Equation (1) is used to approximately account for multiple scattering from the pressure release upper surface and from the lower boundary. The series can be used to generate a sequence of successively more accurate approximations to the true solution. The sequence of approximate solutions is developed in the following analysis.

The equation for the Green's function can be rewritten in the form

$$\begin{aligned} G(\vec{R}_{obs}|\vec{R}_{sp}) &= G_0(\vec{R}_{obs}|\vec{R}_{sp}) + \\ &\int_{S_{UPPER}} [G_0(\vec{R}_{UPPER}|\vec{R}_{sp}) \nabla_{R_{UPPER}} G(\vec{R}_{obs}|\vec{R}_{UPPER})] \cdot \vec{n}_{fl} dS \\ &+ \int_{S_{LOWER}} [G_0(\vec{R}_{LOWER}|\vec{R}_{sp}) \nabla_{R_{LOWER}} G(\vec{R}_{obs}|\vec{R}_{LOWER}) + \\ &G(\vec{R}_{obs}|\vec{R}_{LOWER}) \nabla_{R_{LOWER}} G_0(\vec{R}_{LOWER}|\vec{R}_{sp})] \cdot \vec{n}_{fl} dS \\ &- \int_V \left[(k^2(z_f) - k_0^2) G_0(\vec{R}_f|\vec{R}_{sp}) G(\vec{R}_f|\vec{R}_{sg}) \right] dV \ , \end{aligned}$$

where R_{obs} is substituted for the term R_{sg}.

The foregoing equation for the Green's function can be written in the form

$$G = G_0 + \mathcal{L}\{G_0; G\} \ ,$$

where the operator $\mathcal{L}$ (bilinear in G_O and G) represents the residual effect of boundary scattering and refraction.

The foregoing equation for the Green's function can be written in the form of solving the foregoing fixed-point problem. Under certain circumstances (i.e., when the right-hand side is a contraction mapping and a starting point can be found in the domain of attration), the problem can be solved by the method of Picard iteration; hence, one generates a sequence of approximations, $G_{[n]}$, to the function G with the hope that the sequence converges to the desired function. Specifically, one starts with G_O and one constructs the sequence

$$\begin{aligned} G_{[0]} &= G_0 \\ G_{[1]} &= G_0 - \mathcal{L}\left\{G_0; G_{[0]}\right\} \\ G_{[2]} &= G_0 - \mathcal{L}\left\{G_0; G_{[1]}\right\} \\ &\vdots \quad\quad \vdots \\ G_{[n+1]} &= G_0 - \mathcal{L}\left\{G_0; G_{[n]}\right\} \ . \\ &\vdots \quad\quad \vdots \end{aligned}$$

This sequence of approximations to the Green's function will, under certain circumstances (unknown at this point), converge. In this context, the baseline approach to be used in the current

study can be thought of as the 0-th order approximation, i.e., the approximation $G_{[0]}$ is used in the kernel of equation (1). While the higher order approximations have not been used directly in this study, the value of this formulation is that it provides a constructive approach for calculating each term of the sequence. In addition, this formulation of the problem provides an analytical framework for the expressions used to generate estimates of multiple scattering effects.

A variant of the lowest order approximation, which is of particular interest in the case of a duct with a hard bottom, is

$$G_S = G_{[0']}(\vec{R}_{obs}|\vec{R}_{sp}) = G_0 + G_{0+} - G_{0-}. \tag{2}$$

This approximation will capture the dominant multiple scattering effects for a target near the pressure release upper boundary. The term G_{O+} is the first image with respect to the bottom, and G_{O-} is the first (out of phase) image with respect to the top. This expression represents a special subsequence, which has been summed in the Neumann series. The refractive terms and the more distant images (an infinite number exist) have been ignored.

In addition to the equation for fluid loading, an equation relating the surface pressures and velocities of the target (possibly elastic) is needed. Although a shell approximation for the linear elastic equations describing the target has been implemented, only rigid targets are used in the present study. The relevant equations have been described by Schenck and Benthien (1989) and are not reproduced here. Instead, this result is simply expressed as the following operator relationship between the functions describing the pressure and velocity:

$$\vec{\nabla} p \cdot \vec{n}_{sh} = \mathcal{F}(p) \ \text{ on } S \ ,$$

where S is the wetted surface of the target. The foregoing equations are solved simultaneously to determine the distribution of velocities and pressures on the surface. In the present instance, the equations reduce to the condition that the velocities normal to the target are zero.

Once the distributions of surface pressures and velocities have been calculated, the scattered field is computed using the following equation

$$\overbrace{P(\vec{R}_{obs}|\vec{R}_{sp})}^{\substack{\text{complete}\\ \text{pressure}\\ \text{field}}} = \overbrace{G(\vec{R}_{obs}|\vec{R}_{sp})}^{\substack{\text{source}\\ \text{field}\\ \text{contribution}}} + \underbrace{\int_{S_{sh}} [\overbrace{P(\vec{R}_{sh}|\vec{R}_{sp})}^{\substack{\text{surface}\\ \text{pressure}}} \nabla_{R_{sh}} \overbrace{G(\vec{R}_{obs}|\vec{R}_{sh})}^{\substack{\text{refractive}\\ \text{Green's}\\ \text{function}}} - \overbrace{G(\vec{R}_{obs}|\vec{R}_{sh})}^{\substack{\text{refractive}\\ \text{Green's}\\ \text{function}}} \nabla_{R_{sh}} \overbrace{P(\vec{R}_{sh}|\vec{R}_{sp})}^{\substack{\text{surface}\\ \text{pressure}}}] \cdot \vec{n}_{sh} dS}_{\text{target field contribution}} \ ,$$

where $\vec{R}_{obs}$ is the location in the field at which the pressure is to be calculated.

The propagation Green's function is given a "normal mode" representation as

$$G(r_f, z_f | r_s, z_s) = \frac{i}{4} \sum_{j=1}^{\infty} C_j H_0^{(2)} \left(r \sqrt{k_0^2 - \lambda_j} \right) \phi_j(z_f) \phi_j(z_s) \ , \tag{3}$$

where (r_s, z_s) and (r_f, z_f) are the cylindrical coordinates (range and depth) of the source point and field point, respectively, of the Green's function.

This equation (3) is substituted into the equations for the scattered field and modal scattering amplitudes are computed. The complete scattered field for a target can be computed as a weighted sum of modes. In those cases for which the Green's function cannot be represented as the sum of residues at simple poles, but rather includes contributions from branch points, the branch line integral is ignored. In all cases, the field at the observation point can hence be written as

$$\begin{aligned} P(\vec{R}_{obs} | \vec{R}_{sp}) &= G(\vec{R}_{obs} | \vec{R}_{sp}) + \\ &\frac{i}{4} \sum_{j=1}^{\infty} C_j \phi_j(z_{obs}) [A_j(\vec{R}_{obs}, \vec{R}_{sp}) - B_j(\vec{R}_{obs}, \vec{R}_{sp})] \ , \end{aligned}$$

where (r_s, z_s) and (r_f, z_f) are the cylindrical coordinates (range and depth) of the source point and field point, respectively, of the Green's function.

$$B_j(\vec{R}_{obs}, \vec{R}_{sp}) = \int_{S_{sh}} H_0^{(2)} \left(r_{obs-sh} \sqrt{k_0^2 - \lambda_j} \right) \phi_j(z_{sh}) \vec{\nabla} P(r_{sh}, z_{sh} | r_{sp}, z_{sp}) \cdot \vec{n}_{sh} dS \ \ ,$$

and where

$$\begin{aligned} A_j(\vec{R}_{obs}, \vec{R}_{sp}) \ = \ & \int_{S_{sh}} P(\vec{R}_{sh} | \vec{R}_{sp}) \sqrt{k_0^2 - \lambda_j} H_0'^{(2)} \left(r_{obs-sh} \sqrt{k_0^2 - \lambda_j} \right) \phi_j(z_{sh}) \alpha_r dS + \\ & \int_{S_{sh}} P(\vec{R}_{sh} | \vec{R}_{sp}) H_0^{(2)} \left(r_{obs-sh} \sqrt{k_0^2 - \lambda_j} \right) \phi_j'(z_{sh}) \alpha_z dS \ . \end{aligned}$$

The expression τ_{obs-sh} is the radial component of τ_{obs-sh}, and the α's are given in terms of the horizontal radial unit vector, the vertical depth unit vector, and the target's outward surface normal unit vector as

$$\alpha_r = \vec{e}_r \cdot \vec{n}_{sh}$$

and where

$$\alpha_z = \vec{e}_z \cdot \vec{n}_{sh}.$$

The interpretation given to the above equation is that the pressure field at the point $\vec{R}_{obs}$ consists of the arrival field *G*, which has not been scattered by the target, and of an arrival scattered by the target, and is represented by the linear combinations of the terms B_j and A_j.

APPARENT TARGET STRENGTH

Knowledge of the scattered field, the source strength, the transmission loss from the source to the phase center of the target, and the transmission loss from the phase center of the target to the receiver location is sufficient to calculate an "apparent target strength" using the sonar equation. The qualifier "apparent" is used to indicate that this calculated quantity will be different from the comparable quantity in a free-field environment. This quantity will, in fact, depend upon the specific locations of the source, the target, and the observer. This inability to treat the target and the environment separately is taken to be a violation of a fundamental premise of the sonar equation. The formula used in the calculations is

$$\begin{aligned} TS_{APPARENT} &= 10\log\left(\frac{I_{scattered\ @1\ meter\ from\ target}}{I_{incident\ @target}}\right) \\ &= 10\log\left(\frac{I_{scattered\ @receiver}}{I_{incident\ @1\ meter\ from\ source}}\right) - (TL_{SRC\ to\ TGT} + TL_{TGT\ to\ RCVR}) , \end{aligned}$$

where

$$TL_{TGT\ to\ RCVR} = 10\log\left(\frac{I_{scattered@receiver}}{I_{scattered@1meterfromtarget}}\right) ,$$

and where

$$TL_{SRC\ to\ TGT} = 10\log\left(\frac{I_{incident@target}}{I_{incident@1meterfromsource}}\right) .$$

INTERMODAL SCATTERING STRENGTH

A useful way to look at the problem of the interaction of a target with its environment is as a transition operator between the complex amplitudes of the ensonifying and scattered modes of the duct. This is a more detailed description of the scattering process than is the "apparent target strength," and it allows for a deeper understanding of the phenomenon. In particular, this formulation of the problem reveals a hidden, approximate relationship between the free-field bistatic target strength and the intermodal transition operator.

Equation (1) can be rewritten symbolically as

$$P(\vec{R}_{sg}|\vec{R}_{sp}) = \mathcal{L}_{srf} \circ G(\vec{R}_{sp}|\vec{R}_{sg}) \ .$$

Then, the surface pressure can be rewritten in the form

$$P(\vec{R}_{srf}|\vec{R}_{sp}) = \frac{i}{4}\sum_{j=1}^{\infty} C_j \sqrt{\frac{2}{\pi r_{0\ inc}\sqrt{k_0^2-\lambda_j}}}\ e^{-i(r_{0\ inc}\sqrt{k_0^2-\lambda_j}-\pi/4)}\phi_j(z_{sp})D_j(\vec{r}_{srf}) \ , \tag{4}$$

where

$$D_j(\vec{r}_{srf}) = \mathcal{L}_{srf}\left\{e^{-i(\frac{\vec{r}_{srf}\cdot\vec{r}_{0\ inc}}{r_{0\ inc}}\sqrt{k_0^2-\lambda_j})}\phi_j(z_{srf})\right\} \ , \tag{5}$$

and where the far-field (Fraunhofer zone beyond the Fresnel zone) approximation

$$r_{srf-sp} \doteq r_{0\ inc} + \frac{\vec{r}_{srf}\cdot\vec{r}_{0\ inc}}{|\vec{r}_{0\ inc}|} \tag{6}$$

has been applied.

Similar approximations made in the case of the scattered field yield the following representation:

$$\begin{aligned} P(\vec{R}_{obs}|\vec{R}_{sp}) &= G(\vec{R}_{obs}|\vec{R}_{sp}) + \\ &\frac{i}{4}\frac{i}{4}e^{i\pi/4}e^{i\pi/4}\sum_{j=1}^{\infty}\sum_{l=1}^{\infty}\sqrt{\frac{2}{\pi r_{0\ obs}\sqrt{k_0^2-\lambda_j}}}e^{-i(r_{0\ obs}\sqrt{k_0^2-\lambda_j})}\sqrt{\frac{2}{\pi r_{0\ inc}\sqrt{k_0^2-\lambda_l}}}\ e^{-i(r_{0\ inc}\sqrt{k_0^2-\lambda_l})} \\ &C_jC_l\phi_j(z_{obs})\phi_l(z_{sp})\phi_j(z_{phase\ center})\phi_l(z_{phase\ center})S_{jl} \ , \end{aligned} \tag{7}$$

where

$$S_{jl} = [E_{jl}(\vec{e}_{0\ inc},\vec{e}_{0\ obs}) - F_{jl}(\vec{e}_{0\ inc},\vec{e}_{0\ obs})]/[\phi_j(z_{phase\ center})\phi_l(z_{phase\ center})] \ ,$$

$$\begin{aligned} &E_{jl}(\vec{e}_{0\ inc},\vec{e}_{0\ obs}) = \\ &\int_{S_{sh}} D_l(\vec{r}_{srf})e^{-i(\frac{\vec{r}_{srf}\cdot\vec{r}_{0\ obs}}{|\vec{r}_{0\ obs}|}\sqrt{k_0^2-\lambda_j})}\left[-i\sqrt{k_0^2-\lambda_j}\phi_j(z_{sh})\alpha_r + \phi_j'(z_{sh})\alpha_z\right]dS \ , \end{aligned}$$

and where

$$F_{jl}(\vec{e}_{0\ inc}, \vec{e}_{0\ obs}) = \int_{S_{sh}} e^{-i\left(\frac{\vec{r}_{srf}\cdot\vec{r}_{0\ obs}}{|\vec{r}_{0\ obs}|}\sqrt{k_0^2-\lambda_j}\right)} \phi_j(z_{sh})\vec{\nabla}D_l(\vec{r}_{srf})\cdot\vec{n}_{sh}dS \quad .$$

The quantity S_{ij} is the (linear, rather than logarithmic) analogue of the free-field target strength, and is called here the "intermodal scattering strength." It is the extent to which this quantity is not a constant function of its indices that determines the seriousness of the violations of the sonar equation, since the sonar equation would require that these terms factor completely out of the double sum. The intermodal scattering strength will also be a symmetric function of its indices by virtue of acoustic reciprocity (the symmetry of the Green's function). Finally, it should be noted that the intermodal scattering strength is a function of the *target physics*, the *target depth* (generally) and the *propagation modes of the environment*. While the intermodal scattering strength matrix need not neglect the Fresnel terms (i.e., use the approximations in equation (6)) in the ranges between the target and its source and observer points, the resulting factorization yields a form for equation (7) that is computationally efficient. Specifically, the expensive part of the computations (i.e., S_{ij}) need only be done once for each incident target aspect and observation angle. The double sum then can be inexpensively computed for any combination of source and observer range and depth.

CALCULATED RESULTS

The case studies of a rigid sphere and an elongated rigid body in simple ducts were chosen to demonstrate the model. While elastic shells are easily treated with this methodology, elasticity adds nothing to the understanding of the issues being addressed in the present report. Two environments were investigated. The elongated rigid body consisted of a right-circular cylinder, with a length-to-diameter ratio of 6.3, which is terminated on each end by a hemisphere. The overall length-to-diameter ratio of the body is thus 7.3. The first environment to be investigated was a channel with a uniform sound speed, a uniform depth, and a hard bottom. The second environment was a channel with a deep sound speed axis that gave rise to convergence zones. The sound speed profile chosen was that corresponding to the Monk canonical sound channel (Monk, 1974).

The first target/environment configuration to be considered was the rigid sphere in the uniform duct. The center of the sphere was on the depth centerline of the duct at a distance of 1000a from the source and $ka \approx 1$. First, the scattered field is calculated along a locus of depths from the surface to the channel bottom and lying at the same range as the source (i.e., along a vertical line containing the source point as detailed in figure 1). It is instructive to compare the apparent target strength calculated from the scattered field from the rigid sphere in an unbounded, uniform environment with that for the sphere in a bounded, uniform channel (figure 2) and also with that in the convergence zone (figure 3). Clearly, the effect of the environmental coupling is stronger for the case of the shallow environment with a hard bottom than for the convergence zone. This effect is believed to be a consequence of the different ranged of modal phase velocities (and, hence, effective incident angles) for the two environments. Specifically, in the case of the convergence zone, the phase velocities associated with the modes carrying most of the energy into and away from the target correspond to angles within ± 1 degree of horizontal. In the case of the shallow duct, on the other hand, the modal phase velocities correspond to much greater angles. It is this essentially bistatic scattering phenomenon that gives rise to the large differences between the apparent target strength in the shallow duct and the free-field target strength.

As a further example, the apparent target strength of the elongated body in the shallow duct is shown in figure 5 for the case $ka \approx 1$. The target sits at end incidence to the direction of ensonification and observation. It is noteworthy that the apparent target strength of the elongated object shows even stronger excursions from the predictions of the sonar equation than does the sphere.

Examples of the importance of multiple scattering is shown in figures 5 through 8. In figures 5 and 6, the apparent target strength is shown for the case of the sphere located at distances of 7a and 2a from the surface, respectively. The effect of multiple scattering was determined to be negligible at the center, but more significant for the target near the surface. Corresponding apparent target strengths are shown in figures 7 and 8 for the target near the rigid bottom.

The effects of neglecting the Fresnel terms implicit in the use of the approximation of equation (6) are shown in figure 9. The case of the elongated body oriented at beam aspect to the source/receiver axis is treated. A comparison of the complete solution with the approximate solution indicates that the effect of being in the Fresnel zone is a second-order effect, but is clearly detectable at moderate ranges.

CONCLUSIONS

Numerical confirmation has been obtained of the significant violations of the sonar equation which can occur in dispersive environments. This problem is shown to be more serious for a shallow water duct having a hard bottom than for a convergence zone environment. A simple interpretation of this phenomenon is that the great range model phase velocities in a shallow duct gives rise to stronger equivalent bistatic effects.

Multiple scattering effects have been shown to be observable for a target near the surface of the duct. They were not significant near the center of the duct under study.

The effects of neglecting Fresnel terms, which makes the problem particularly efficient to solve, are not entirely negligible at useful ranges.

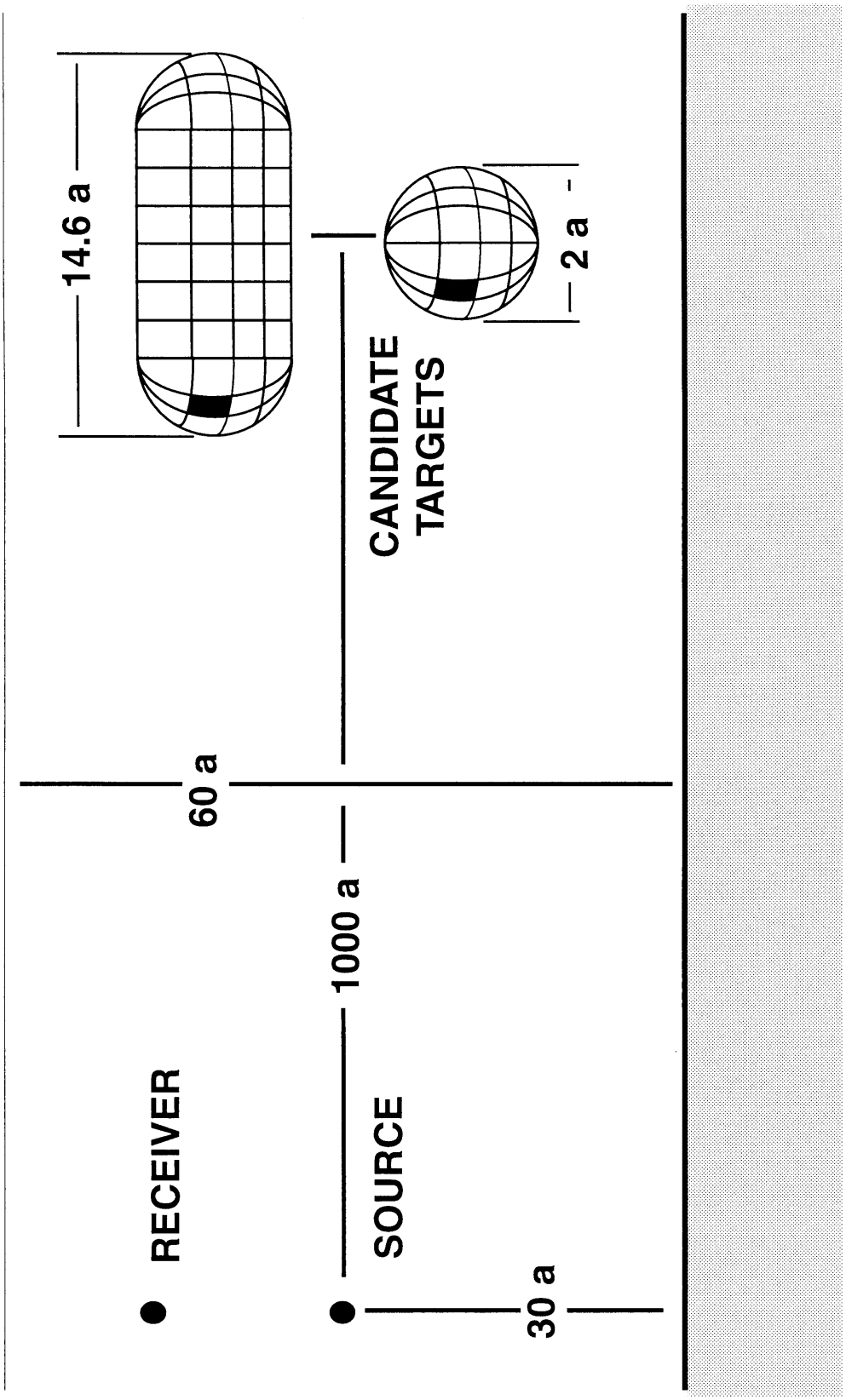

Figure 1. Source/target/receiver arrangement for shallow duct.

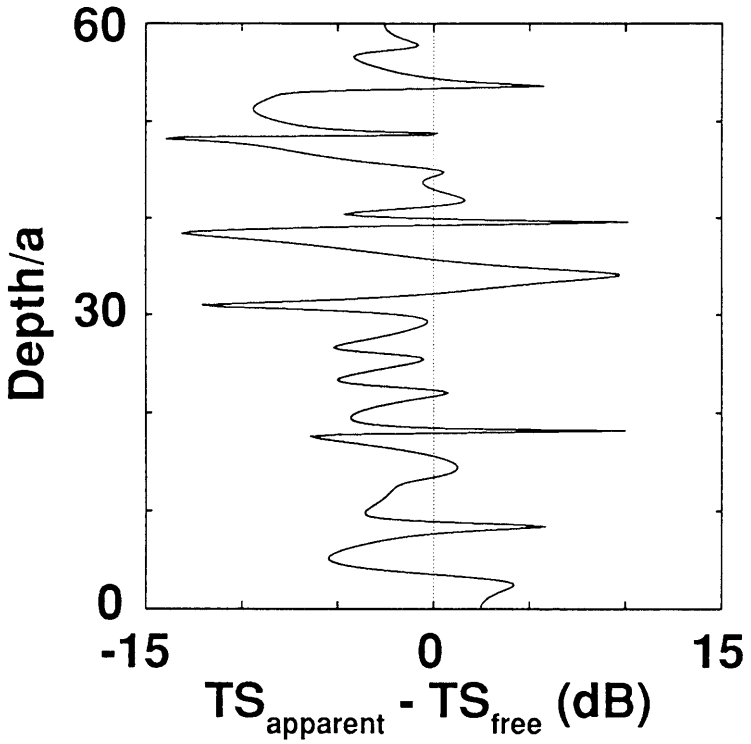

Figure 2. Apparent target strength of hard sphere in uniform duct with hard bottom.

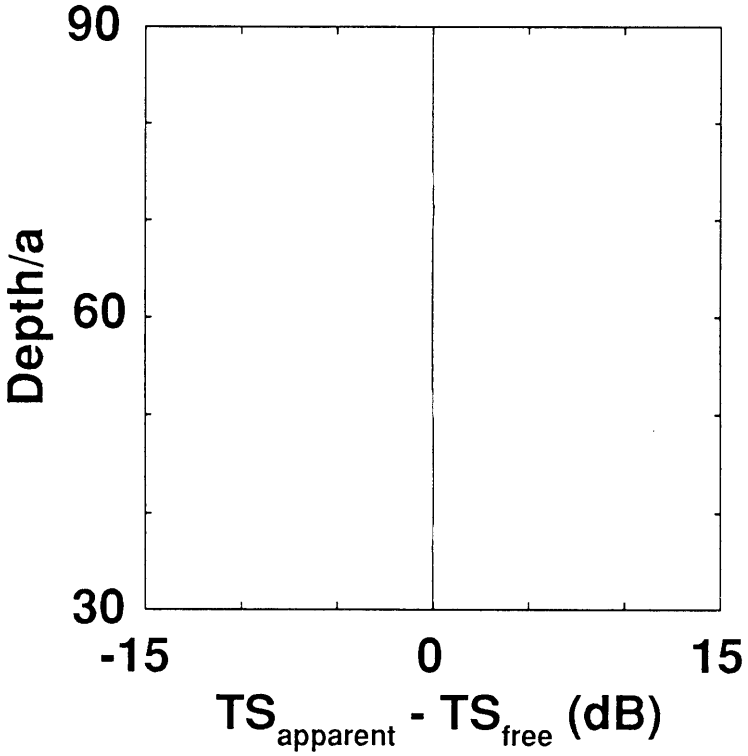

Figure 3. Apparent target strength of hard sphere in convergence zone.

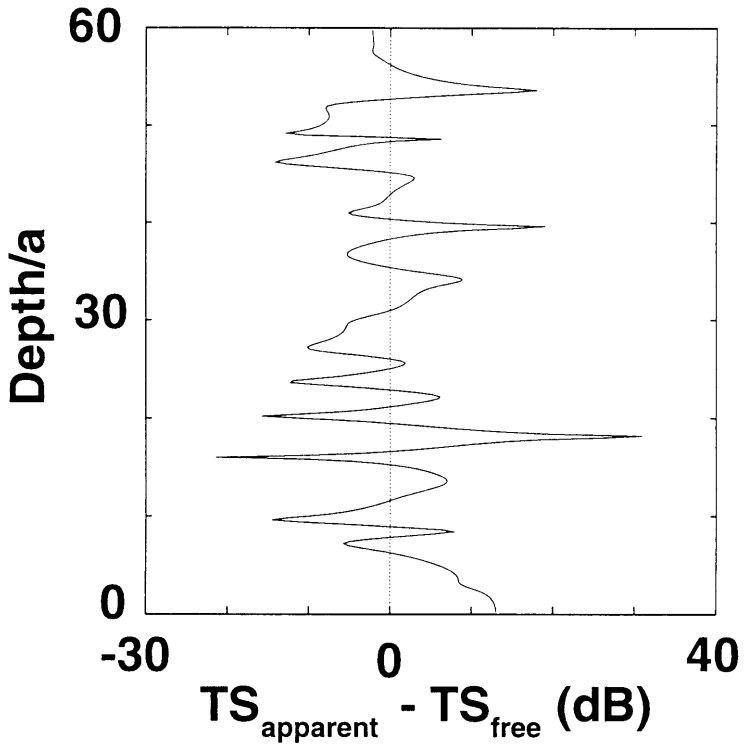

Figure 4. Apparent target strength of rigid cylinder in duct. End Aspect.

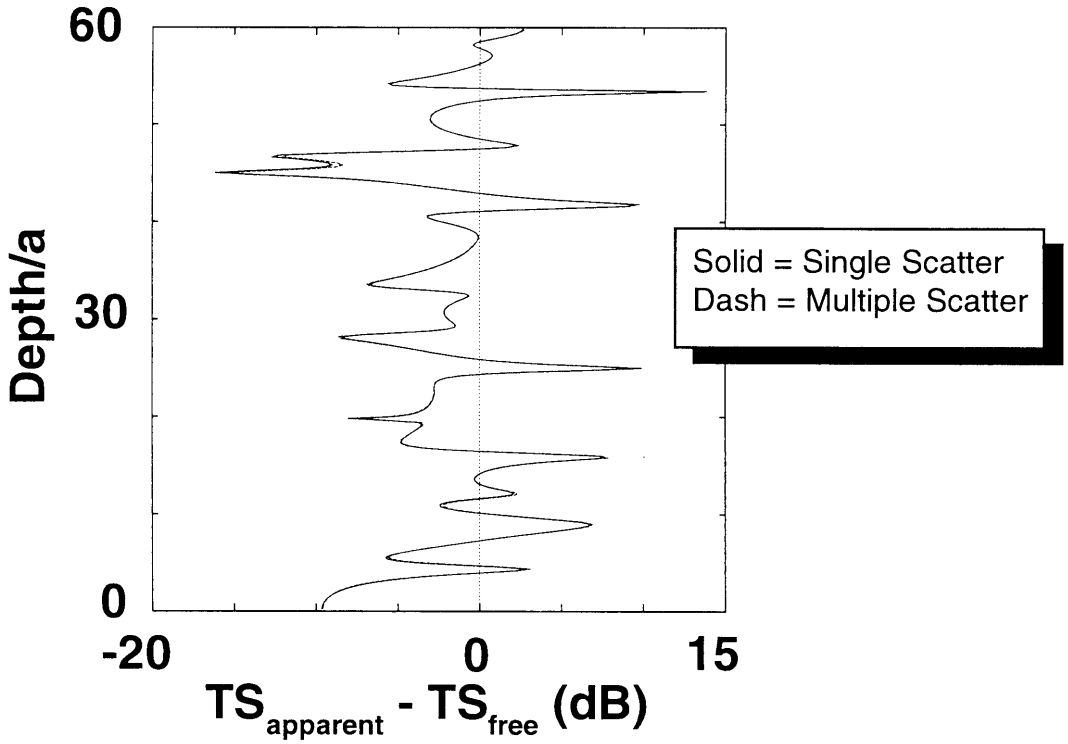

Figure 5. Multiple scattering effects on apparent target strength of rigid sphere near surface. Target depth/a = 7.

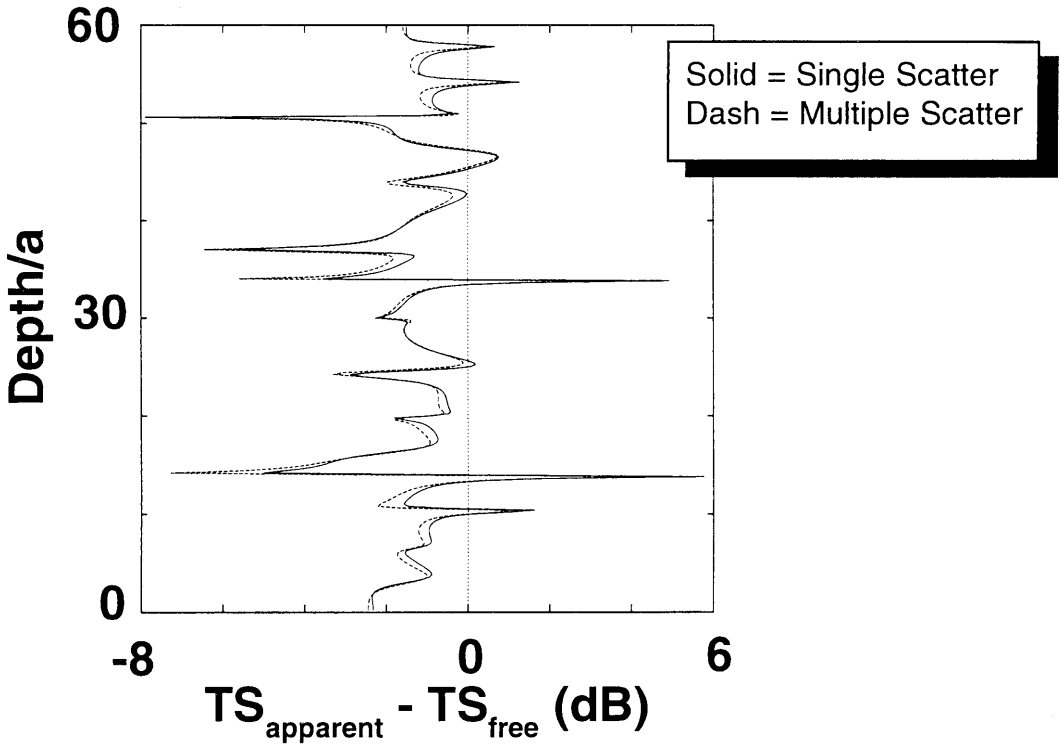

Figure 6. Multiple scattering effects on apparent target strength of rigid sphere near surface. Target Depth/a = 2.

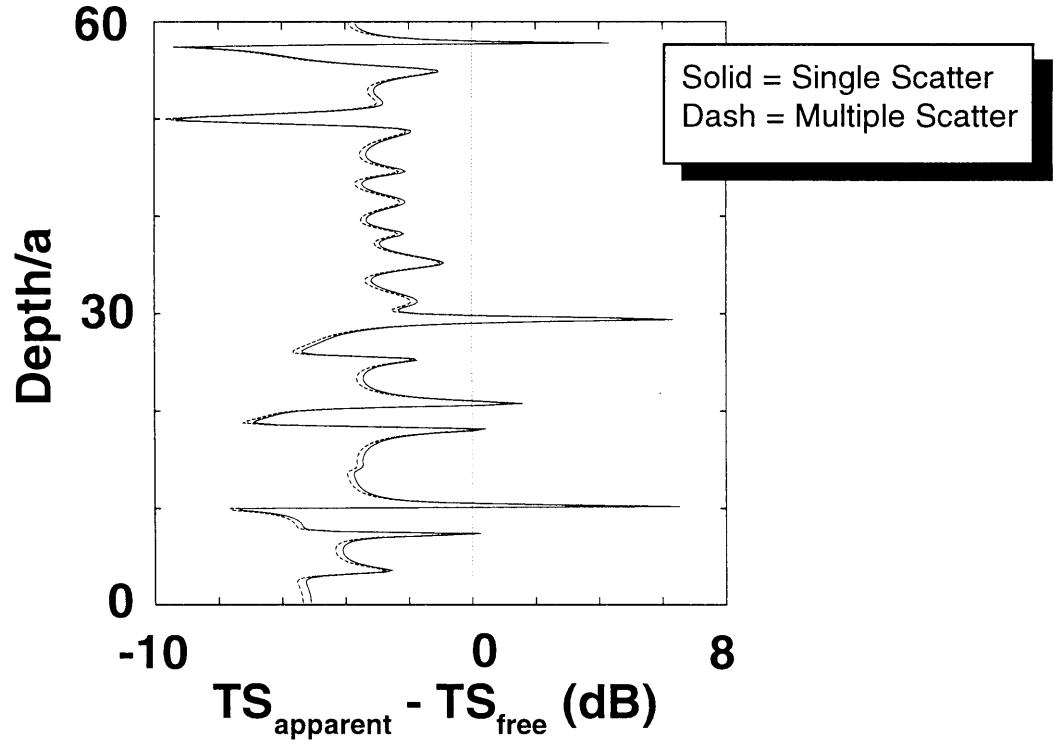

Figure 7. Multiple scattering effects on apparent target strength of rigid sphere near rigid bottom. Target depth/a = 53.

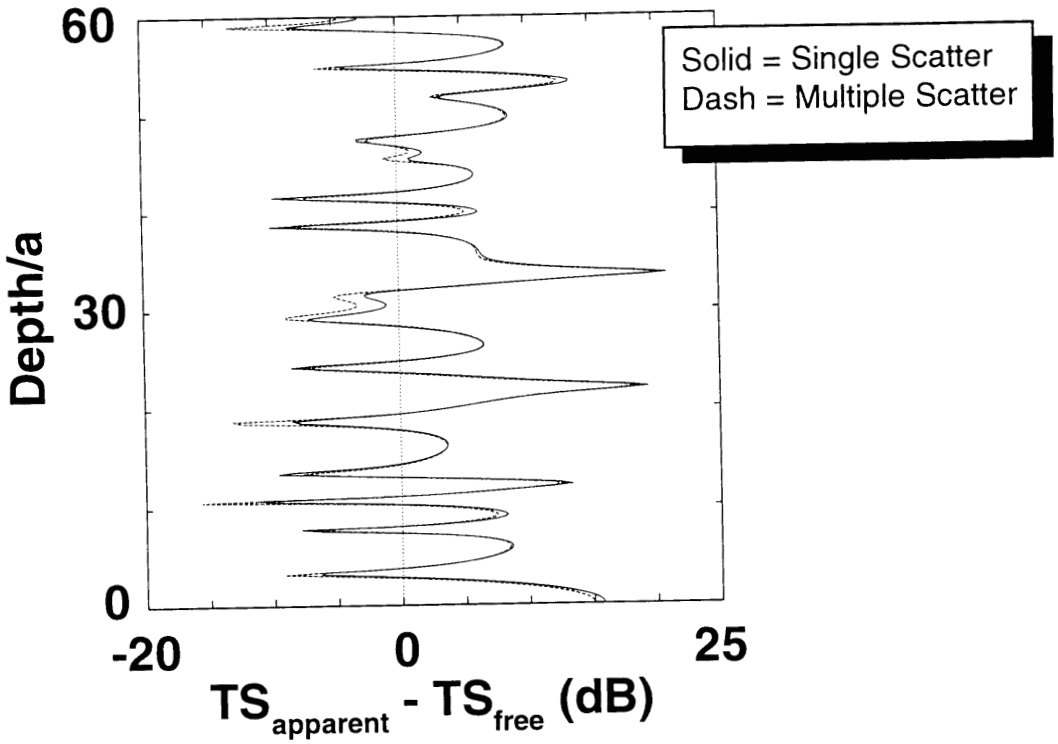

Figure 8. Multiple scattering effects on apparent target strength of rigid sphere near hard bottom. Target Depth/a = 58.

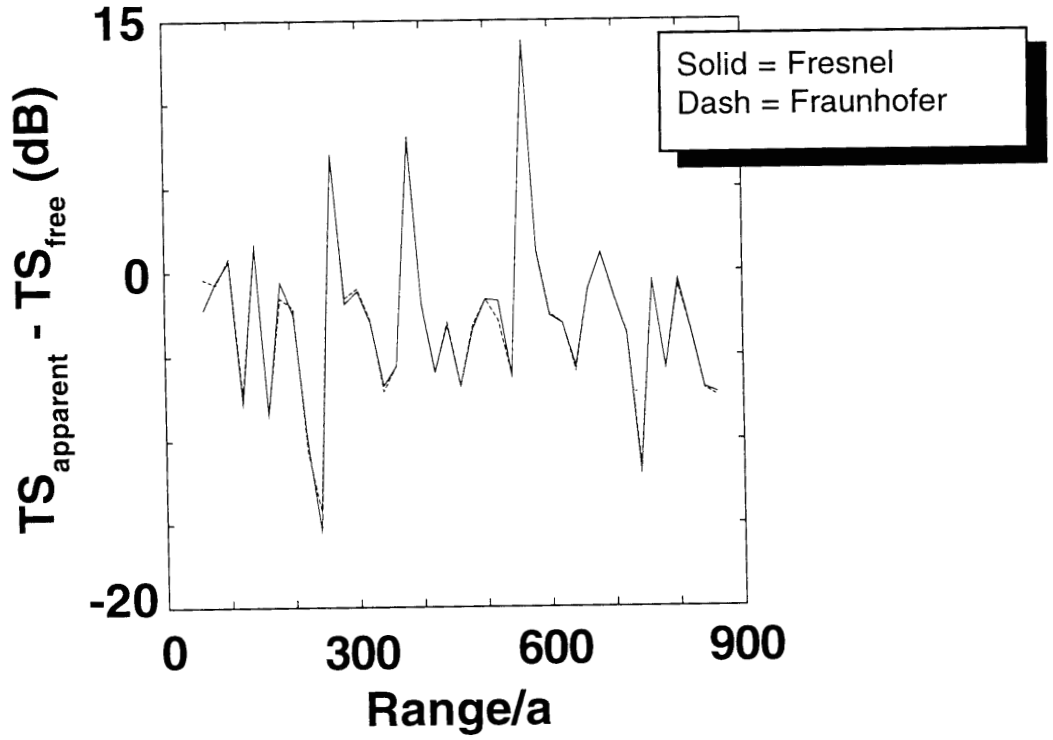

Figure 9. Effect of Fresnel terms on apparent target strength for rigid cylinder with end caps. Target at center of duct and at beam aspect.

REFERENCES (U)

McDaid, E. P., D. Gillette, and D. Barach. 1992. *The Scattering of Sound from a Target in a Non-uniform Environment*. TR 1519, (Sep). Naval Command, Control and Ocean Surveillance Center, RDT&E Div., San Diego, CA.

Schenck, H. A. and G. W. Benthien. 1989. *Numerical Solution of Acoustic-Structure Interaction Problems*. TR 1263, (Apr). Naval Ocean Systems Center, San Diego, CA.

Munk, W. H. 1974. Sound channel in an exponentially stratified ocean, with application to SOFAR. *Journal of the Acoustical Society of America*, 55(2):220–226.

APPENDIX

EQUATION DERIVATIONS

A.1 FORMULATION OF THE PROBLEM

This appendix is a generalized version of equation derivations detailed by McDaid et al. (1992). The general approach in solving this problem is to use a version of the Helmholtz Integral Equation that has been modified to account for the refractive acoustic environment in combination with a so-called normal mode formulation of the acoustic propagation. The refractive Green's function is used to calculate the pressure incident on the wetted surface of the shell. The baseline, free-field version of the Helmholtz Integral Equation is then used to calculate the pressures and velocities on the wetted surface (equation A.6). Finally, the refractive version of the Helmholtz Integral Equation is used to calculate the far-field scattered pressure (equation A.5). The modal representation of the refractive Green's function (equation A.9) makes the problem particuarly easy to formulate.

A.2 EXTERIOR HELMHOLTZ EQUATION FOR REFRACTIVE ENVIRONMENT

The formulation of the scattering problem for a shell in a refractive environment in which the sound speed profile is horizontally stratified is straightforward, since it is so similar to the equivalent problem in a uniform acoustic medium. The derivation of the relevant equations is included herein for the sake of completeness, rather than as a demonstration of their novelty. Throughout this work, the time dependence of the signals is assumed to be e^{iwt}. The domain of interest is a half space, *V,* with a pressure release boundary condition at the surface, S_{UPPER}. Let the vectors $\vec{R}_{fg}$ and $\vec{R}_{sg}$ be the field and source points for the Green's function for the following boundary value problem

$$\left[\nabla^2_{R_{fg}} + k^2(z_{fg})\right] G(\vec{R}_{fg}|\vec{R}_{sg}) = -\delta(\vec{R}_{fg} - \vec{R}_{sg}) \text{ in } V \ ,$$
$$G(\vec{R}_{fg}|\vec{R}_{sg}) = 0 \text{ on } S_{UPPER} \ ,$$

and

$$\lim_{r_g \to \infty} r_g \left| \frac{\partial G}{\partial r} + ikG \right| = 0,$$

where $\tau_g = |\vec{R}_{fg} - \vec{R}_{sg}|$, and $k(z_{fg}) = \omega/c(z_{fg}$. The term $\vec{n}_{fl}$ is the outward normal on the fluid body at the shell surface, S_{sh}. Note that $\vec{n}_{fl} = -\vec{n}_{sh}$, where $\vec{n}_{sh}$ is the outward normal to the elastic shell, and

$$\lim_{\vec{R}_{fg} \to \vec{R}_{sg}} \left[G(\vec{R}_{fg}|\vec{R}_{sg}) - \frac{e^{-ik|\vec{R}_{fg} - \vec{R}_{sg}|}}{4\pi|\vec{R}_{fg} - \vec{R}_{sg}|} \right] = 0.$$

This last equation is used to justify the use of the free-space Green's function in equation (A.6) as an approximation of G. Also note that the Green's function is symmetric, i.e., $G(\vec{R}_{fg}|\vec{R}_{sg}) = G(\vec{R}_{sg}|\vec{R}_{fg})$.

Let the vectors $\vec{R}_{fp}$ and $\vec{R}_{sp}$ be the field and source points for the pressure in the following boundary value problem

$$\left[\nabla^2_{R_{fp}} + k^2(z_{fp})\right] P(\vec{R}_{fp}|\vec{R}_{sp}) = 0 \text{ in } V \ ,$$

$$P(\vec{R}_{fp}|\vec{R}_{sp}) = 0 \text{ on } S_{UPPER} \ ,$$

$$\vec{\nabla}_{R_{fp}} P(\vec{R}_{fp}|\vec{R}_{sp}) \cdot \vec{n}_{fl} = \mathcal{F}[P(\vec{R}_{fp}|\vec{R}_{sp})] \ \ on \ \ S_{sh} \ ,$$

and

$$\lim_{r_p \to \infty} r_p | \frac{\partial P}{\partial r} + ikP | = 0 \ ,$$

where $\tau_p = |\vec{R}_{fp} - \vec{R}_{sp}|$, $k(z_{fp}) = \omega / c(z_{fp})$, and S_{sh} is the wetted surface of the elastic shell. The functional relationship $\mathcal{F}$ is used to embody the effect of the elastic shell. Note that $\mathcal{F}$ is a mapping between functions.

In the present example, let $\vec{R}_{fp} = \vec{R}_{fg} = \vec{R}_f$. We then have the result

$$P(\vec{R}_f|\vec{R}_{sp}) \left[\nabla^2_{R_f} + k^2(z_f)\right] G(\vec{R}_f|\vec{R}_{sg}) - G(\vec{R}_f|\vec{R}_{sg}) \left[\nabla^2_{R_f} + k^2(z_f)\right] P(\vec{R}_f|\vec{R}_{sp}) = 0 \ ,$$

and

$$P(\vec{R}_f|\vec{R}_{sp}) \nabla^2_{R_f} G(\vec{R}_f|\vec{R}_{sg}) - G(\vec{R}_f|\vec{R}_{sg}) \nabla^2_{R_f} P(\vec{R}_f|\vec{R}_{sp}) = 0 \ . \qquad \text{(A.1)}$$

The following identities are useful in simplifying the foregoing expression:

$$\begin{aligned} \nabla_{R_f} \cdot [P(\vec{R}_f|\vec{R}_{sp}) \nabla_{R_f} G(\vec{R}_f|\vec{R}_{sg})] = \ & \nabla_{R_f} P(\vec{R}_f|\vec{R}_{sp}) \cdot \nabla_{R_f} G(\vec{R}_f|\vec{R}_{sg}) + \\ & P(\vec{R}_f|\vec{R}_{sp}) \nabla^2_{R_f} G(\vec{R}_f|\vec{R}_{sg}) = 0 \ , \end{aligned}$$

and

$$\begin{aligned} \nabla_{R_f} \cdot [G(\vec{R}_f|\vec{R}_{sg}) \nabla_{R_f} P(\vec{R}_f|\vec{R}_{sp})] = \ & \nabla_{R_f} G(\vec{R}_f|\vec{R}_{sg}) \cdot \nabla_{R_f} P(\vec{R}_f|\vec{R}_{sp}) + \\ & G(\vec{R}_f|\vec{R}_{sg}) \nabla^2_{R_f} P(\vec{R}_f|\vec{R}_{sp}) = 0 \ . \end{aligned}$$

Hence, equation (A.1) can be written in a simplified form as

$$\nabla_{R_f} \cdot [P(\vec{R}_f|\vec{R}_{sp}) \nabla_{R_f} G(\vec{R}_f|\vec{R}_{sg}) - G(\vec{R}_f|\vec{R}_{sg}) \nabla_{R_f} P(\vec{R}_f|\vec{R}_{sp})] = 0.$$

This expression can be integrated over the volume, which excludes the shell and its interior, a tiny sphere of radius ε centered at R_{sp}, and another tiny sphere or radius ε centered at R_{sg}. Since there are no sources in this volume, one has the result

$$\int_{V-V_{\epsilon g}-V_{\epsilon p}-V_{sh}} \nabla_{R_f} \cdot [P(\vec{R}_f|\vec{R}_{sp})\nabla_{R_f} G(\vec{R}_f|\vec{R}_{sg}) - G(\vec{R}_f|\vec{R}_{sg})\nabla_{R_f} P(\vec{R}_f|\vec{R}_{sp})]dV = 0.$$

This is readily converted into a surface integral of the form

$$\int_{S_{\epsilon g}+S_{\epsilon p}+S_{sh}} [P(\vec{R}_f|\vec{R}_{sp})\nabla_{R_f} G(\vec{R}_f|\vec{R}_{sg}) - G(\vec{R}_f|\vec{R}_{sg})\nabla_{R_f} P(\vec{R}_f|\vec{R}_{sp})] \cdot \qquad \text{(A.2)}$$

The integrals over the surfaces S_{eg} and S_{ep} have particularly simple limiting forms. Note that

$$\begin{aligned}
\int_{S_{\epsilon g}} P(\vec{R}_f|\vec{R}_{sp})\nabla_{R_f} G(\vec{R}_f|\vec{R}_{sg}) \cdot \vec{n}_{fl} dS &\doteq P(\vec{R}_{sg}|\vec{R}_{sp}) \int_{S_{\epsilon g}} \nabla_{R_f} G(\vec{R}_f|\vec{R}_{sg}) \cdot \vec{n}_{fl} dS \\
&\doteq P(\vec{R}_{sg}|\vec{R}_{sp}) \left[-(4\pi\epsilon^2) \frac{\partial}{\partial \epsilon} \left(\frac{e^{-ik\epsilon}}{4\pi\epsilon} \right) \right] \\
&\doteq P(\vec{R}_{sg}|\vec{R}_{sp}) \left[-(4\pi\epsilon^2) \left(-ik \frac{e^{-ik\epsilon}}{4\pi\epsilon} - \frac{e^{-ik\epsilon}}{4\pi\epsilon^2} \right) \right] \\
&\doteq P(\vec{R}_{sg}|\vec{R}_{sp}) \ .
\end{aligned}$$

Similarly, one has

$$\begin{aligned}
\int_{S_{\epsilon p}} G(\vec{R}_f|\vec{R}_{sg})\nabla_{R_f} P(\vec{R}_f|\vec{R}_{sp}) \cdot \vec{n}_{fl} dS &\doteq G(\vec{R}_{sp}|\vec{R}_{sg}) \int_{S_{\epsilon p}} \nabla_{R_f} P(\vec{R}_f|\vec{R}_{sp}) \cdot \vec{n}_{fl} dS \\
&\doteq G(\vec{R}_{sp}|\vec{R}_{sg}) [-(4\pi\epsilon^2) \frac{\partial}{\partial \epsilon} \left(\frac{e^{-ik\epsilon}}{4\pi\epsilon} \right)] \\
&\doteq G(\vec{R}_{sp}|\vec{R}_{sg}) \left[-(4\pi\epsilon^2) \left(-ik \frac{e^{-ik\epsilon}}{4\pi\epsilon} - \frac{e^{-ik\epsilon}}{4\pi\epsilon^2} \right) \right] \\
&\doteq G(\vec{R}_{sp}|\vec{R}_{sg}) \ .
\end{aligned}$$

Note also that

$$\begin{aligned}
\int_{S_{\epsilon g}} G(\vec{R}_f|\vec{R}_{sg})\nabla_{R_f} P(\vec{R}_f|\vec{R}_{sp}) \cdot \vec{n}_{fl} dS &\doteq |\nabla_{R_f} P(\vec{R}_{sg}|\vec{R}_{sp})| \int_{S_{\epsilon p}} G(\vec{R}_f|\vec{R}_{sg}) \vec{e} \cdot \vec{n}_{fl} dS \\
&\doteq |\nabla_{R_f} P(\vec{R}_{sg}|\vec{R}_{sp})| \frac{1}{4\pi\epsilon} \int_{S_{\epsilon p}} \vec{e} \cdot \vec{n}_{fl} dS \\
&\doteq 0.
\end{aligned}$$

Similarly, one has

$$\begin{aligned}\int_{S_{\epsilon p}} P(\vec{R}_f|\vec{R}_{sp})\nabla_{R_f} G(\vec{R}_f|\vec{R}_{sg})\cdot\vec{n}_{fl}dS &\doteq |\nabla_{R_f} G(\vec{R}_{sp}|\vec{R}_{sg})|\int_{S_{\epsilon g}} P(\vec{R}_f|\vec{R}_{sp})\vec{e}\cdot\vec{n}_{fl}dS \\ &\doteq |\nabla_{R_f} G(\vec{R}_{sp}|\vec{R}_{sg})|\frac{1}{4\pi\epsilon}\int_{S_{\epsilon g}}\vec{e}\cdot\vec{n}_{fl}dS \\ &\doteq 0.\end{aligned}$$

These four approximations are exact in the limit as ε shrinks to 0. The surface integral can thus be written as

$$\begin{aligned}&P(\vec{R}_{sg}|\vec{R}_{sp}) - G(\vec{R}_{sp}|\vec{R}_{sg}) + \\ &\quad\int_{S_{sh}}[P(\vec{R}_{sh}|\vec{R}_{sp})\nabla_{R_{sh}} G(\vec{R}_{sh}|\vec{R}_{sg}) - G(\vec{R}_{sh}|\vec{R}_{sg})\nabla_{R_{sh}} P(\vec{R}_{sh}|\vec{R}_{sp})]\cdot\vec{n}_{fl}dS = 0.\end{aligned} \tag{A.3}$$

The surface integral can thus be rewritten in terms of the shell normal as

$$\begin{aligned}&P(\vec{R}_{obs}|\vec{R}_{sp}) = G(\vec{R}_{obs}|\vec{R}_{sp}) + \\ &\quad\int_{S_{sh}}[P(\vec{R}_{sh}|\vec{R}_{sp})\nabla_{R_{sh}} G(\vec{R}_{obs}|\vec{R}_{sh}) - G(\vec{R}_{obs}|\vec{R}_{sh})\nabla_{R_{sh}} P(\vec{R}_{sh}|\vec{R}_{sp})]\cdot\vec{n}_{sh}dS\ ,\end{aligned} \tag{A.4}$$

A change of notation can be invoked and the symmetry of the Green's function can be used to cast the problem into a form familiar to those working in scattering theory, such that

$$\begin{aligned}&P(\vec{R}_{obs}|\vec{R}_{sp}) = G(\vec{R}_{obs}|\vec{R}_{sp}) + \\ &\quad\int_{S_{sh}}[P(\vec{R}_{sh}|\vec{R}_{sp})\nabla_{R_{sh}} G(\vec{R}_{obs}|\vec{R}_{sh}) - G(\vec{R}_{obs}|\vec{R}_{sh})\nabla_{R_{sh}} P(\vec{R}_{sh}|\vec{R}_{sp})]\cdot\vec{n}_{sh}dS\ ,\end{aligned} \tag{A.5}$$

where R_{obs} is substituted for the term R_{sg}.

The interpretation of the above result is that the resulting field consists of the direct arrival from the source, represented by *G*, and a term scattered off the shell and represented by the surface integrals over the shell surface.

A.3 EXTERIOR HELMHOLTZ EQUATION WITH REFRACTIVE ENVIRONMENT AND LIQUID BOTTOM

In the case of a "liquid bottom," one has essentially two different media with which to deal. It is most correct to specify the propagation in terms of two Green's functions, one for each of the media. The Pekeris duct is a special case of this situation. In this section, we will use the convention of calling these functions G_1 and G_2 for the Green's functions in the surface layer and basement layer, respectively. The analysis for this case follows that of the single medium very closely. The difference is that boundary conditions at the liquid-liquid interface must be satisfied. These results are easily extended to the case of a multilayer liquid layer.

The target will always be assumed to lie in the surface layer. An equation corresponding to equation (A.2), but applying in the surface layer, is

$$\int_{S_{\epsilon g}+S_{\epsilon p}+S_{sh}+S_b} [P_1(\vec{R}_f|\vec{R}_{sp})\nabla_{R_f} G_1(\vec{R}_f|\vec{R}_{sg}) - G_1(\vec{R}_f|\vec{R}_{sg})\nabla_{R_f} P_1(\vec{R}_f|\vec{R}_{sp})] \cdot \vec{n}_{fl1} dS = 0.$$

The subscript *fl1* refers to the outward normal on the surface layer at the interface, and the subscript *b* refers to the surface. Similarly, one has, for the field in the basement layer, the equation

$$\int_{S_{\epsilon g}+S_{\epsilon p}+S_b} [P_2(\vec{R}_f|\vec{R}_{sp})\nabla_{R_f} G_2(\vec{R}_f|\vec{R}_{sg}) - G_2(\vec{R}_f|\vec{R}_{sg})\nabla_{R_f} P_2(\vec{R}_f|\vec{R}_{sp})] \cdot \vec{n}_{fl2} dS = 0.$$

The subscript *fl2* refers to the outward normal on the basement layer. In the foregoing equations, provision has been made for the possibility of the source and field points lying in either of the two layers.

The two media are coupled through the acoustic boundary conditions which obtain at the interface, i.e., the equality of stress

$$G_1(\vec{R}_f|\vec{R}_{sg}) = G_2(\vec{R}_f|\vec{R}_{sg}) \ ,$$

and the equality of normal velocities

$$\nabla_{R_f} G_1(\vec{R}_f|\vec{R}_{sg}) \cdot \vec{n}_{fl1}/\rho_1 = -\nabla_{R_f} G_2(\vec{R}_f|\vec{R}_{sg}) \cdot \vec{n}_{fl2}/\rho_2 \ ,$$

where it is noted that $\vec{n}_{fl1} = -\vec{n}_{fl2}$.

Similarly, the pressure fields satisfy the same boundary conditions

$$P_1(\vec{R}_f|\vec{R}_{sg}) = P_2(\vec{R}_f|\vec{R}_{sg})$$

and the equality of normal velocities

$$\nabla_{R_f} P_1(\vec{R}_f|\vec{R}_{sg}) \cdot \vec{n}_{fl1}/\rho_1 = -\nabla_{R_f} P_2(\vec{R}_f|\vec{R}_{sg}) \cdot \vec{n}_{fl2}/\rho_2 \ .$$

A complete treatment of the sound field would require that a number of cases be considered, in accordance with the layers in which the source and field points lie. In this study, the most important case (and the only one for which calculations will be done) is that one in which both $\vec{R}_{sg}$ and $\vec{F}_{sp}$ lie in the surface layer.

The equations for the pressures in the two media become as follows:

$$P_1(\vec{R}_{sg}|\vec{R}_{sp}) - G_1(\vec{R}_{sp}|\vec{R}_{sg}) + \int_{S_{sh}} [P_1(\vec{R}_{sh}|\vec{R}_{sp})\nabla_{R_{sh}} G_1(\vec{R}_{sh}|\vec{R}_{sg}) - G_1(\vec{R}_{sh}|\vec{R}_{sg})\nabla_{R_{sh}} P_1(\vec{R}_{sh}|\vec{R}_{sp})] \cdot \vec{n}_{fl} dS + \int_{S_b} [P_1(\vec{R}_b|\vec{R}_{sp})\nabla_{R_b} G_1(\vec{R}_b|\vec{R}_{sg}) - G_1(\vec{R}_b|\vec{R}_{sg})\nabla_{R_b} P_1(\vec{R}_b|\vec{R}_{sp})] \cdot \vec{n}_{fl1} dS = 0 \ ,$$

and the equality of normal velocities

$$\int_{S_b} [P_2(\vec{R}_b|\vec{R}_{sp})\nabla_{R_b} G_2(\vec{R}_b|\vec{R}_{sg}) - G_2(\vec{R}_b|\vec{R}_{sg})\nabla_{R_b} P_2(\vec{R}_b|\vec{R}_{sp})] \cdot \vec{n}_{fl2} dS = 0.$$

Using the interface boundary conditions, one has

$$\begin{aligned} 0 &= \int_{S_b} [P_2(\vec{R}_b|\vec{R}_{sp})\nabla_{R_b} G_2(\vec{R}_b|\vec{R}_{sg}) - G_2(\vec{R}_b|\vec{R}_{sg})\nabla_{R_b} P_2(\vec{R}_b|\vec{R}_{sp})] \cdot \vec{n}_{fl2} dS \\ &= \int_{S_b} [P_1(\vec{R}_b|\vec{R}_{sp})\nabla_{R_b} \left[\frac{-\rho_2}{\rho_1}\right] G_1(\vec{R}_b|\vec{R}_{sg}) - G_1(\vec{R}_b|\vec{R}_{sg}) \left[\frac{-\rho_2}{\rho_1}\right] \nabla_{R_b} P_1(\vec{R}_b|\vec{R}_{sp})] \cdot \vec{n}_{fl2} dS \\ &= \frac{-\rho_2}{\rho_1} \int_{S_b} [P_1(\vec{R}_b|\vec{R}_{sp})\nabla_{R_b} G_1(\vec{R}_b|\vec{R}_{sg}) - G_1(\vec{R}_b|\vec{R}_{sg})\nabla_{R_b} P_1(\vec{R}_b|\vec{R}_{sp})] \cdot \vec{n}_{fl1} dS \end{aligned}$$

If one substitutes this latter result into the equation for P_1, then one has the expected result, which is equivalent to equation (A.3).

$$\begin{aligned} &P_1(\vec{R}_{sg}|\vec{R}_{sp}) - G_1(\vec{R}_{sp}|\vec{R}_{sg}) + \\ &\int_{S_{sh}} [P_1(\vec{R}_{sh}|\vec{R}_{sp})\nabla_{R_{sh}} G_1(\vec{R}_{sh}|\vec{R}_{sg}) - G_1(\vec{R}_{sh}|\vec{R}_{sg})\nabla_{R_{sh}} P_1(\vec{R}_{sh}|\vec{R}_{sp})] \cdot \vec{n}_{fl} dS = 0. \end{aligned}$$

By using the appropriate change of notation and invoking the symmetry of the Green's function, one arrives at an equation identical to equation (A.5).

A.4 SURFACE INTEGRAL EQUATION

In this case, perform the same analysis, except that one lets $\vec{R}_{sg}$ be on the surface of the shell. In this case, one has the equation

$$\begin{aligned} &\frac{1}{2} P(\vec{R}_{sg}|\vec{R}_{sp}) = G(\vec{R}_{sp}|\vec{R}_{sg}) + \\ &\int_{S_{sh}} [P(\vec{R}_{sh}|\vec{R}_{sp})\nabla_{R_{sh}} G(\vec{R}_{sh}|\vec{R}_{sg}) - G(\vec{R}_{sh}|\vec{R}_{sg})\nabla_{R_{sh}} P(\vec{R}_{sh}|\vec{R}_{sp})] \cdot \vec{n}_{sh} dS \ . \end{aligned}$$

It is this equation that must be solved in order to evaluate the pressure and velocity on the surface of the shell. In the present instance, the approximation is used in which the free-field propagation Green's function is used *within* the integral, rather than the actual refractive Green's function. The *forcing* function, $G(\vec{R}_{sp}|\vec{R}_{sg})$, for the integral equation is, however, the actual refractive Green's function. More will be said regarding this approximation in section A.11. For the sake of clarity, this integral equation can be rewritten in terms of the free-field Green's function G_O as

$$\begin{aligned} &\frac{1}{2} P(\vec{R}_{sg}|\vec{R}_{sp}) = G(\vec{R}_{sp}|\vec{R}_{sg}) + \\ &\int_{S_{sh}} [P(\vec{R}_{sh}|\vec{R}_{sp})\nabla_{R_{sh}} G_0(\vec{R}_{sh}|\vec{R}_{sg}) - G_0(\vec{R}_{sh}|\vec{R}_{sg})\nabla_{R_{sh}} P(\vec{R}_{sh}|\vec{R}_{sp})] \cdot \vec{n}_{sh} dS \ . \end{aligned} \tag{A.6}$$

If one denotes the inverse of the foregoing integral operator by the symbol $\mathcal{L}_{STf}$, then

$$P(\vec{R}_{sg}|\vec{R}_{sp}) = \int_{S_{sh}} K(\vec{R}'_{sg}, \vec{R}_{sp}; \vec{R}_{sg}) G(\vec{R}_{sp}|\vec{R}'_{sg}) dS(\vec{R}'_{sg}) \ ,$$

or

$$P(\vec{R}_{sg}|\vec{R}_{sp}) = \mathcal{L}_{srf} G(\vec{R}_{sp}|\vec{R}_{sg}) \ .$$

A.5 NORMAL MODE REPRESENTATION OF PROPAGATION GREEN's FUNCTION

In the present study, two categories of stratified sound speed profiles have been considered. In the first instance, an approximate solution has been found for the so-called "Pekeris" wave guide. This environment consists of two fluid layers, each with a uniform density and sound speed. The upper layer is finite in depth and is bounded above by a pressure release boundary. The lower layer is an infinite half space. In the second instance, a multilayer environment is chosen in which propagation exhibits convergence zone behavior. The sound speed is a continuous function of depth. Within each layer, the square of the sound speed has a hyperbolic dependence on depth. In the deepest layer, which is an infinite half-space, the sound speed has an asymptotic limiting value of zero.

The propagation Green's function is a solution to the following boundary value problem

$$\left[\nabla^2_{R_{fg}} + k^2(z_{fg})\right] G(\vec{R}_{fg}|\vec{R}_{sg}) = -\delta(\vec{R}_{fg} - \vec{R}_{sg}) \text{ in } V \ ,$$

$$G(\vec{R}_{fg}|\vec{R}_{sg}) = 0 \text{ on } S_{UPPER} \ ,$$

$$\lim_{r_g \to \infty} r_g \left|\frac{\partial G}{\partial r_g} + ikG\right| = 0 \ ,$$

where r_g is the *horizontal* separation distance between $\vec{R}_{fg}$ and $\vec{R}_{sg}$. In the case of a horizontally stratified sound speed profile, it is convenient to solve the sound propagation problem in cylindrical coordinates. In those cases where the Green's function can be represented as a series of eigenfunction products or a residue series, without the inclusion of a branch line integral contribution, one has

$$G(r_f, z_f|r_s, z_s) = \frac{i}{4} \sum_{j=1}^{\infty} H_0^{(2)}(r\sqrt{k_0^2 - \lambda_j}) G_z(z_f|z_s; -\lambda_j) \ ,$$

where the summation is over a discrete set of values of the (complex) separation parameter λ, where r is the *horizontal* separation between $\vec{R}_f$ and $\vec{R}_s$, and where k_0 is a reference wave number. The choice of a value for k_0 is dependent on the sound speed profile being considered in a particular application.

In the present work, a standard notation will always be used when defining cylindrincal coordinate systems. The depth coordinate z will always be positive downward, so $\vec{e}_z$ will point down.

The radial coordinate *r* will be *horizontal*, and the following subscripting notation will be used for *r* and the horizontal radial unit vector $\vec{e}_r$:

$$r_{f-s} = |(\vec{R}_f - \vec{R}_s) - [(\vec{R}_f - \vec{R}_s) \cdot \vec{e}_z]\vec{e}_z| \tag{A.7}$$

and

$$\vec{e}_r = |(\vec{R}_f - \vec{R}_s) - [(\vec{R}_f - \vec{R}_s) \cdot \vec{e}_z]\vec{e}_z|/r_{f-s} \ . \tag{A.8}$$

The depth Green's function, G_z, is further written as

$$G_z(z_f|z_s; -\lambda_j) = C_j \phi_j(z_f)\phi_j(z_s) \ ,$$

where the function $\phi_j(z)$ is the j-th depth "eigenfunction." The reason for temporizing with regard to the name of the function ϕ_j is that the series is actually a residue series in the cases of certain sound speed profiles, and it is not clear if the functions should be considered an orthonormal basis for the function space under consideration since they may not be integrable. The functions ϕ_j have been chosen such that $\phi_j(0) = 0$ and $\partial\phi j/\partial z = -1$ for $z = 0$, where the depth *z* is a positive quantity and has a value of 0 at the surface.

By substituting this result into the original equation for the Green's function, one has

$$G(r_f, z_f|r_s, z_s) = \frac{i}{4}\sum_{j=1}^{\infty} C_j H_0^{(2)}(r\sqrt{k_0^2 - \lambda_j})\phi_j(z_f)\phi_j(z_s) \ . \tag{A.9}$$

The gradient of the Green's function is given as

$$\begin{aligned} \vec{\nabla}G(r_f, z_f|r_s, z_s) = \frac{i}{4}\sum_{j=1}^{\infty} C_j \\ [\vec{e}_r\sqrt{k_0^2 - \lambda_j}H_0^{\prime(2)}\left(r\sqrt{k_0^2 - \lambda_j}\right)\phi_j(z_f)\phi_j(z_s) + \\ \vec{e}_z H_0^{(2)}\left(r\sqrt{k_0^2 - \lambda_j}\right)\phi_j'(z_f)\phi_j(z_s)] \ . \end{aligned} \tag{A.10}$$

The horizontal radian unit vector $\vec{e}_r$ points away from the source point, and the axial unit vector $\vec{e}_z$ points down, since hte sign convention will be that *z* is depth, and hence, increases in the downward direction (equations A.7 and A.8).

The expression for the surface pressure can hence be rewritten as

$$P(\vec{R}_{srf}|\vec{R}_{sp}) = \frac{i}{4}\sum_{j=1}^{\infty} C_j \mathcal{L}_{srf}\left\{H_0^{(2)}(r_{srf-sp}\sqrt{k_0^2 - \lambda_j})\phi_j(z_{srf})\right\}\phi_j(z_{sp}) \ .$$

Using the asymptotic representation of the Hankel function, one has

$$P(\vec{R}_{srf}|\vec{R}_{sp}) = \frac{i}{4}\sum_{j=1}^{\infty} C_j \mathcal{L}_{srf}\left\{\sqrt{\frac{2}{\pi r\sqrt{k_0^2 - \lambda_j}}}\ e^{-i(r_{srf-sp}\sqrt{k_0^2-\lambda_j}-\pi/4)}\phi_j(z_{srf})\right\}\phi_j(z_{sp}) \ .$$

Let the location of the phase center of the scatterer be denoted $\vec{R}_{phase\ center}$ and let

$$\vec{r}_{0\ inc} = \vec{R}_{phase\ center} - \vec{R}_{sp} - [(\vec{R}_{phase\ center} - \vec{R}_{sp}) \cdot \vec{e}_z]\vec{e}_z$$

be the vector from the source point to the phase center of the target. Let

$$\vec{r}_{srf} = \vec{R}_{srf} - \vec{R}_{phase\ center} - [(\vec{R}_{srf} - \vec{R}_{phase\ center}) \cdot \vec{e}_z]\vec{e}_z$$

be the vector from the phase center of the scatterer to the surface point. The following approximation is used for large values of the horizontal range from the source point to the surface point, r_{srf-sp},

$$r_{srf-sp} \doteq r_{0\ inc} + \frac{\vec{r}_{srf} \cdot \vec{r}_{0\ inc}}{|\vec{r}_{0\ inc}|} \ ,$$

where $\vec{r}_{0\ inc}$ is the vector pointing from the source point to the phase center of the target, and $r_{0\ inc} = |\vec{r}_{0\ inc}|$. The pressure can be written approximately as

$$P(\vec{R}_{srf}|\vec{R}_{sp}) = \frac{i}{4}\sum_{j=1}^{\infty} C_j \mathcal{L}_{srf}\left\{\sqrt{\frac{2}{\pi r_{0\ inc}\sqrt{k_0^2-\lambda_j}}}\ e^{-i(r_{0\ inc}\sqrt{k_0^2-\lambda_j}-\pi/4)}\ e^{-i(\vec{r}_{srf}\cdot\frac{\vec{r}_{0\ inc}}{r_{0\ inc}}\sqrt{k_0^2-\lambda_j})}\phi_j(z_{srf})\right\}\phi_j(z_{sp}) \ .$$

An approximate "modal factorization" can be performed as follows:

$$P(\vec{R}_{srf}|\vec{R}_{sp}) = \frac{i}{4}\sum_{j=1}^{\infty} C_j \sqrt{\frac{2}{\pi r_{0\ inc}\sqrt{k_0^2-\lambda_j}}}\ e^{-i(r_{0\ inc}\sqrt{k_0^2-\lambda_j}-\pi/4)}\phi_j(z_{sp})\mathcal{L}_{srf}\left\{e^{-i(\frac{\vec{r}_{srf}\cdot\vec{r}_{0\ inc}}{r_{0\ inc}}\sqrt{k_0^2-\lambda_j})}\phi_j(z_{srf})\right\} \ ,$$

or

$$P(\vec{R}_{srf}|\vec{R}_{sp}) = \frac{i}{4}\sum_{j=1}^{\infty} C_j \sqrt{\frac{2}{\pi r_{0\ inc}\sqrt{k_0^2-\lambda_j}}}\ e^{-i(r_{0\ inc}\sqrt{k_0^2-\lambda_j}-\pi/4)}\phi_j(z_{sp})D_j(\vec{r}_{srf}) \ , \qquad \text{(A.11)}$$

where

$$D_j(\vec{r}_{srf}) = \mathcal{L}_{srf}\left\{e^{-i(\frac{\vec{r}_{srf}\cdot\vec{r}_{0\ inc}}{r_{0\ inc}}\sqrt{k_0^2-\lambda_j})}\phi_j(z_{srf})\right\} \ . \qquad \text{(A.11)}$$

Equation (A.11) is simply the surface pressure that has been calculated by using CHIEF/MART-SAM for the case of a point source located at $\vec{R}_{sp}$. Equation (A.12), on the other hand, is the surface pressure that would be calculated by using the partial point source strength that is given by

$$e^{-i(\frac{\vec{r}_{srf}\cdot\vec{r}_{0\ inc}}{r_{0\ inc}}\sqrt{k_0^2-\lambda_j})}\phi_j(z_{srf}) \ ,$$

rather than the entire source strength $G(\vec{R}_{srf}|\vec{R}_{sp})$.

Similar results can be obtained for the gradient of the surface pressure, i.e.,

$$\vec{\nabla} P(\vec{R}_{srf}|\vec{R}_{sp}) = \frac{i}{4}\sum_{j=1}^{\infty} C_j \sqrt{\frac{2}{\pi r_{0\ inc}\sqrt{k_0^2-\lambda_j}}}\ e^{-i(r_{0\ inc}\sqrt{k_0^2-\lambda_j}-\pi/4)}\phi_j(z_{sp})\vec{\nabla}\mathcal{L}_{srf}\left\{e^{-i(\frac{\vec{r}_{srf}\cdot\vec{r}_{0\ inc}}{r_{0\ inc}}\sqrt{k_0^2-\lambda_j})}\phi_j(z_{srf})\right\}\ ,$$

or

$$\vec{\nabla} P(\vec{R}_{srf}|\vec{R}_{sp}) = \frac{i}{4}\sum_{j=1}^{\infty} C_j \sqrt{\frac{2}{\pi r_{0\ inc}\sqrt{k_0^2-\lambda_j}}}\ e^{-i(r_{0\ inc}\sqrt{k_0^2-\lambda_j}-\pi/4)}\phi_j(z_{sp})\vec{\nabla} D_j(\vec{r}_{srf})\ .$$

The errors in this expression are $O(1/r_{0\,inc})$.

A.6 MODAL REPRESENTATION OF SCATTERED PRESSURE

By substituting equation (A.9) and equation (A.10) in equation (A.5), the two surface integrals can now be evaluated in terms of quadratures involving the depth eigenfunctions. In particular, one has

$$\int_{S_{sh}} G(\vec{R}_{obs}|\vec{R}_{sh})\nabla_{R_{sh}} P(\vec{R}_{sh}|\vec{R}_{sp})\cdot\vec{n}_{sh}dS = \frac{i}{4}\sum_{j=1}^{\infty} C_j\phi_j(z_{obs})B_j(\vec{R}_{obs},\vec{R}_{sp})\ ,$$

where

$$B_j(\vec{R}_{obs},\vec{R}_{sp}) = \int_{S_{sh}} H_0^{(2)}(r_{obs-sh}\sqrt{k_0^2-\lambda_j})\phi_j(z_{sh})\vec{\nabla} P(r_{sh},z_{sh}|r_{sp},z_{sp})\cdot\vec{n}_{sh}dS\ \ ,$$

and $r_{obs–sh}$ is defined in accordance with the conventions of equations (A.7) and (A.8).

Similarly, one has

$$\int_{S_{sh}} P(\vec{R}_{sh}|\vec{R}_{sp})\nabla_{R_{sh}} G(\vec{R}_{obs}|\vec{R}_{sh})\cdot\vec{n}_{sh}dS = \frac{i}{4}\sum_{j=1}^{\infty} C_j\phi_j(z_{obs})A_j(\vec{R}_{obs},\vec{R}_{sp})\ ,$$

where

$$A_j(\vec{R}_{obs},\vec{R}_{sp}) = \int_{S_{sh}} P(\vec{R}_{sh}|\vec{R}_{sp})\sqrt{k_0^2-\lambda_j}H_0'^{(2)}(r_{obs-sh}\sqrt{k_0^2-\lambda_j})\phi_j(z_{sh})\alpha_r dS + \int_{S_{sh}} P(\vec{R}_{sh}|\vec{R}_{sp})H_0^{(2)}(r_{obs-sh}\sqrt{k_0^2-\lambda_j})\phi_j'(z_{sh})\alpha_z dS\ ,$$

and where the α's are given in terms of the unit *horizontal* radial vector and the unit vertical depth vector as

$$\alpha_r = \vec{e}_r\cdot\vec{n}_{sh}\ ,$$

and

$$\alpha_z = \vec{e}_z \cdot \vec{n}_{sh} \ .$$

It is clear from equations (A.4) and (A.10) that the radial unit vector must point *away* from $\vec{R}_{obs}$..

The following asymptotic approximations of the Hankel function and its derivative are used in the calculations (equations 9.2.4 and 9.1.28 of Abramowitz & Stegun (1964))

$$H_0^{(2)}(x) \sim \sqrt{\frac{2}{\pi x}} \ e^{-i(x-\pi/4)} \ ,$$

where

$$H_0'^{(2)}(x) \sim -i\sqrt{\frac{2}{\pi x}} \ e^{-i(x-\pi/4)}.$$

The field at the observation point can, hence, be written as

$$\begin{aligned} P(\vec{R}_{obs}|\vec{R}_{sp}) &= G(\vec{R}_{obs}|\vec{R}_{sp}) + \\ &\frac{i}{4}\sum_{j=1}^{\infty} C_j \phi_j(z_{obs})[A_j(\vec{R}_{obs},\vec{R}_{sp}) - B_j(\vec{R}_{obs},\vec{R}_{sp})] \ . \end{aligned} \tag{A.13}$$

The interpretation given to the above equation is that the pressure field at the point $\vec{R}_{obs}$ consists of the arrival field *G*, which has not been scattered by the target, and of an arrival scattered by the shell and represented by the linear combinations of the terms B_j and A_j.

Using the approximate modal factorization, one has

$$\begin{aligned} A_j(\vec{R}_{obs},\vec{R}_{sp}) = \frac{i}{4}\sum_{l=1}^{\infty} C_l \sqrt{\frac{2}{\pi r_{0\ inc}\sqrt{k_0^2-\lambda_l}}} \ e^{-i(r_{0\ inc}\sqrt{k_0^2-\lambda_l}-\pi/4)}\phi_l(z_{sp}) \\ \left\{ \int_{S_{sh}} D_l(\vec{r}_{srf})\sqrt{k_0^2-\lambda_j} H_0'^{(2)}(r_{obs-sh}\sqrt{k_0^2-\lambda_j})\phi_j(z_{sh})\alpha_r dS + \right. \\ \left. \int_{S_{sh}} D_l(\vec{r}_{srf}) H_0^{(2)}(r_{obs-sh}\sqrt{k_0^2-\lambda_j})\phi_j'(z_{sh})\alpha_z dS \right\} \ , \end{aligned}$$

or

$$\begin{aligned} A_j(\vec{R}_{obs},\vec{R}_{sp}) = \frac{i}{4} e^{i\pi/4} e^{i\pi/4} \sqrt{\frac{2}{\pi r_{obs-sh}\sqrt{k_0^2-\lambda_j}}} \\ \sum_{l=1}^{\infty} C_l \sqrt{\frac{2}{\pi r_{0\ inc}\sqrt{k_0^2-\lambda_l}}} \ e^{-i(r_{0\ inc}\sqrt{k_0^2-\lambda_l})}\phi_l(z_{sp}) \\ \int_{S_{sh}} D_l(\vec{r}_{srf}) e^{-i(r_{obs-sh}\sqrt{k_0^2-\lambda_j})} \left[-i\sqrt{k_0^2-\lambda_j}\phi_j(z_{sh})\alpha_r + \phi_j'(z_{sh})\alpha_z \right] dS \ . \end{aligned}$$

Let

$$\vec{r}_{obs} = \vec{R}_{phase\ center} - \vec{R}_{obs} - [(\vec{R}_{phase\ center} - \vec{R}_{obs}) \cdot$$

be the vector from the field point, where the scattered pressure is being calculated, to the phase center of the scatterer. Use the approximation

$$r \doteq r_{0\ obs} + \frac{\vec{r}_{srf} \cdot \vec{r}_{0\ obs}}{|\vec{r}_{0\ obs}|} \ ,$$

where $r_{0\ inc} = |\vec{r}_{0\ inc}|$ to get the result

$$A_j(\vec{R}_{obs}, \vec{R}_{sp}) = \frac{i}{4} e^{i\pi/4} e^{i\pi/4} \sqrt{\frac{2}{\pi r_{obs-sh} \sqrt{k_0^2 - \lambda_j}}}$$
$$\sum_{l=1}^{\infty} C_l \sqrt{\frac{2}{\pi r_{0\ inc} \sqrt{k_0^2 - \lambda_l}}}\ e^{-i(r_{0\ inc}\sqrt{k_0^2-\lambda_l})} \phi_l(z_{sp})$$
$$\int_{S_{sh}} D_l(\vec{r}_{srf}) e^{-i(r_{obs-sh}\sqrt{k_0^2-\lambda_j})} \left[-i\sqrt{k_0^2 - \lambda_j}\phi_j(z_{sh})\alpha_r + \phi_j'(z_{sh})\alpha_z \right] dS \ .$$

This result can be written with simplified notation as

$$A_j(\vec{R}_{obs}, \vec{R}_{sp}) = \frac{i}{4} e^{i\pi/4} e^{i\pi/4} \sqrt{\frac{2}{\pi r_{0\ obs} \sqrt{k_0^2 - \lambda_j}}} e^{-i(r_{0\ obs}\sqrt{k_0^2-\lambda_j})}$$
$$\sum_{l=1}^{\infty} C_l \sqrt{\frac{2}{\pi r_{0\ inc} \sqrt{k_0^2 - \lambda_l}}}\ e^{-i(r_{0\ inc}\sqrt{k_0^2-\lambda_l})} \phi_l(z_{sp}) E_{jl}(\vec{e}_{0\ inc}, \vec{e}_{0\ obs}) \ ,$$

where

$$E_{jl}(\vec{e}_{0\ inc}, \vec{e}_{0\ obs}) =$$
$$\int_{S_{sh}} D_l(\vec{r}_{srf}) e^{-i(\frac{\vec{r}_{srf}\cdot\vec{r}_{0\ obs}}{|\vec{r}_{0\ obs}|}\sqrt{k_0^2-\lambda_j})} \left(-i\sqrt{k_0^2 - \lambda_j}\phi_j(z_{sh})\alpha_r + \phi_j'(z_{sh})\alpha_z \right) dS \ .$$

Similar approximations can be found for the terms B_j:

$$B_j(\vec{R}_{obs}, \vec{R}_{sp}) = \frac{i}{4} e^{i\pi/4} e^{i\pi/4} \sqrt{\frac{2}{\pi r_{0\ obs} \sqrt{k_0^2 - \lambda_j}}} e^{-i(r_{0\ obs}\sqrt{}}$$
$$\sum_{l=1}^{\infty} C_l \phi_l(z_{sp}) \sqrt{\frac{2}{\pi r_{0\ inc} \sqrt{k_0^2 - \lambda_l}}}\ e^{-i(r_{0\ inc}\sqrt{k_0^2-\lambda_l})}$$
$$\int_{S_{sh}} e^{-i(\frac{\vec{r}_{srf}\cdot\vec{r}_{0\ obs}}{|\vec{r}_{0\ obs}|}\sqrt{k_0^2-\lambda_j})} \phi_j(z_{sh}) \vec{\nabla} D_l(\vec{r}_{srf}) \cdot \vec{n}_{sh} dS \ ,$$

or

$$B_j(\vec{R}_{obs},\vec{R}_{sp}) = \frac{i}{4}e^{i\pi/4}e^{i\pi/4}\sqrt{\frac{2}{\pi r_{0\ obs}\sqrt{k_0^2-\lambda_j}}}e^{-i(r_{0\ obs}\sqrt{k_0^2-\lambda_j})}$$
$$\sum_{l=1}^{\infty} C_l\phi_l(z_{sp})\sqrt{\frac{2}{\pi r_{0\ inc}\sqrt{k_0^2-\lambda_l}}}\ e^{-i(r_{0\ inc}\sqrt{k_0^2-\lambda_l})}F_{jl}(\vec{e}_{0\ inc},\vec{e}_{0\ obs})\ ,$$

where

$$F_{jl}(\vec{e}_{0\ inc},\vec{e}_{0\ obs}) =$$
$$\int_{S_{sh}} e^{-i(\frac{\vec{r}_{srf}\cdot\vec{r}_{0\ obs}}{|\vec{r}_{0\ obs}|}\sqrt{k_0^2-\lambda_j})}\phi_j(z_{sh})\vec{\nabla}D_l(\vec{r}_{srf})\cdot\vec{n}_{sh}dS\ .$$

The scattered pressure (equation A.13) can be rewritten as

$$P(\vec{R}_{obs}|\vec{R}_{sp}) = G(\vec{R}_{obs}|\vec{R}_{sp})+$$
$$\frac{i}{4}\frac{i}{4}e^{i\pi/4}e^{i\pi/4}\sum_{j=1}^{\infty}\sum_{l=1}^{\infty}\sqrt{\frac{2}{\pi r_{0\ obs}\sqrt{k_0^2-\lambda_j}}}e^{-i(r_{0\ obs}\sqrt{k_0^2-\lambda_j})}\sqrt{\frac{2}{\pi r_{0\ inc}\sqrt{k_0^2-\lambda_l}}}\ e^{-i(r_{0\ inc}\sqrt{k_0^2-\lambda_l})}$$
$$C_jC_l\phi_j(z_{obs})\phi_l(z_{sp})[E_{jl}(\vec{e}_{0\ inc},\vec{e}_{0\ obs}) - F_{jl}(\vec{e}_{0\ inc},\vec{e}_{0\ obs})]\ .$$

It is the quantities $E_{jl}(\vec{e}_{0\ inc},\vec{e}_{0\ obs})$ and $F_{jl}(\vec{e}_{0\ inc},\vec{e}_{0\ obs})$ that are the fundamental scattering coefficients which must be calculated. The analogue of a target strength, call it the "cross-modal target strength," or the "inter-modal target strength," can be written as

$$TS_{jl} = [E_{jl}(\vec{e}_{0\ inc},\vec{e}_{0\ obs}) - F_{jl}(\vec{e}_{0\ inc},\vec{e}_{0\ obs})]/[\phi_j(z_{phase\ center})\phi_l(z_{phase\ center})]\ .$$

The equation for the scattered pressure can thus be written as

$$P(\vec{R}_{obs}|\vec{R}_{sp}) = G(\vec{R}_{obs}|\vec{R}_{sp})+$$
$$\frac{i}{4}\frac{i}{4}e^{i\pi/4}e^{i\pi/4}\sum_{j=1}^{\infty}\sum_{l=1}^{\infty}\sqrt{\frac{2}{\pi r_{0\ obs}\sqrt{k_0^2-\lambda_j}}}e^{-i(r_{0\ obs}\sqrt{k_0^2-\lambda_j})}\sqrt{\frac{2}{\pi r_{0\ inc}\sqrt{k_0^2-\lambda_l}}}\ e^{-i(r_{0\ inc}\sqrt{k_0^2-\lambda_l})}$$
$$C_jC_l\phi_j(z_{obs})\phi_l(z_{sp})\phi_j(z_{phase\ center})\phi_l(z_{phase\ center})TS_{jl}\ .$$

A.7 NUMERICAL APPROXIMATIONS

In the version of the CHIEF/MARTSAM software to be used, an approximation is to be used in which surface elements S_n, are assumed to have constant pressure and normal velocity. In this case, B_j and A_j, appearing in equation (A.13) have the following representations:

$$B_{jn}(\vec{R}_{obs},\vec{R}_{sp}) = \int_{S_n}\sqrt{\frac{2}{\pi(r_{obs-sh}\sqrt{k_0^2-\lambda_j})}}e^{-i\left[(r_{obs-sh}\sqrt{k_0^2-\lambda_j})-\pi/4\right]}$$
$$\phi_j(z_{sh})\vec{\nabla}P(r_{sh},z_{sh}|r_{sp},z_{sp})\cdot\vec{n}_{sh}dS\ .$$

This can be rewritten approximately as

$$\begin{aligned} B_{jn}(\vec{R}_{obs},\vec{R}_{sp}) &= \vec{\nabla}P(r_{shn},z_{shn}|r_{sp},z_{sp})\cdot\vec{n}_{shn}\ \ e^{i\pi/4} \\ &\quad \int_{S_n}\sqrt{\frac{2}{\pi(r_{obs-sh}\sqrt{k_0^2-\lambda_j})}}e^{-i(r_{obs-sh}\sqrt{k_0^2-\lambda_j})}\phi_j(z_{sh})dS \\ &= -i\omega\rho_n V_n e^{i\pi/4}Q_{vjn}\ . \end{aligned}$$

The total expression for B_j is

$$B_j(\vec{R}_{obs},\vec{R}_{sp}) = -i\omega e^{i\pi/4}\sum_{n=1}^{N}\rho_n V_n(\vec{R}_{sp})Q_{vjn}(\vec{R}_{obs})\ \ .$$

In the case of the coefficients A_j, one has

$$\begin{aligned} &A_{jn}(\vec{R}_{obs},\vec{R}_{sp}) = \\ &\quad \int_{S_n}P(\vec{R}_{sh}|\vec{R}_{sp})\sqrt{k_0^2-\lambda_j}\left\{-i\sqrt{\frac{2}{\pi(r_{obs-sh}\sqrt{k_0^2-\lambda_j})}}e^{-i\left[(r_{obs-sh}\sqrt{k_0^2-\lambda_j})-\pi/4\right]}\right\}\phi_j(z_{sh})\alpha_r dS + \\ &\quad \int_{S_n}P(\vec{R}_{sh}|\vec{R}_{sp})\sqrt{\frac{2}{\pi(r_{obs-sh}\sqrt{k_0^2-\lambda_j})}}e^{-i\left[(r_{obs-sh}\sqrt{k_0^2-\lambda_j})-\pi/4\right]}\phi_j'(z_{sh})\alpha_z dS\ \ . \end{aligned}$$

This can be rewritten as

$$\begin{aligned} A_{jn}(\vec{R}_{obs},\vec{R}_{sp}) &= \int_{S_n}P(\vec{R}_{sh}|\vec{R}_{sp})e^{-i\left[(r_{obs-sh}\sqrt{k_0^2-\lambda_j})-\pi/4\right]}\sqrt{\frac{2}{\pi(r_{obs-sh}\sqrt{k_0^2-\lambda_j})}} \\ &\quad [-i\sqrt{k_0^2-\lambda_j}\phi_j(z_{sh})\alpha_r+\phi_j'(z_{sh})\alpha_z]dS\ \ . \end{aligned}$$

As before, this again can be rewritten in the approximate form

$$\begin{aligned} A_{jn}(\vec{R}_{obs},\vec{R}_{sp}) &= P(\vec{R}_{sh}|\vec{R}_{sp})e^{i\pi/4}\int_{S_n}e^{-i(r_{obs-sh}\sqrt{k_0^2-\lambda_j})}\sqrt{\frac{2}{\pi(r_{obs-sh}\sqrt{k_0^2-\lambda_j})}} \\ &\quad \left[-i\sqrt{k_0^2-\lambda_j}\phi_j(z_{sh})\alpha_r+\phi_j'(z_{sh})\alpha_z\right]dS \\ &= P_n e^{i\pi/4}Q_{pjn}\ \ . \end{aligned}$$

The total expression for A_j is

$$A_j(\vec{R}_{obs},\vec{R}_{sp}) = e^{i\pi/4}\sum_{n=1}^{N}P_n(\vec{R}_{sp})Q_{pjn}(\vec{R}_{obs})\ \ .$$

There is a rough correspondence between the coefficients $B_j(\vec{R}_{obs},\vec{R}_{sp})$ and $A_j(\vec{R}_{obs},\vec{R}_{sp})$ and the coefficients B_{ff} and A_{ff} as used in the formulation of the baseline CHIEF/MARTSAM software. That correspondence is as follows:

$$B_j(\vec{R}_{obs}, \vec{R}_{sp}) \Longleftrightarrow \frac{e^{-ikR}}{R} B_{ff}(x,n) \ ,$$

and

$$A_j(\vec{R}_{obs}, \vec{R}_{sp}) \Longleftrightarrow \frac{e^{-ikR}}{R} A_{ff}(x,n) \ .$$

A noteworthy difference between the baseline version of the CHIEF/MARTSAM software and the case of the refractive environment is that in the latter case, one cannot extract a simple factor which will account for the propagation loss of the scattered wave away from the shell.

The expression for the total resulting field generated by the source in the presence of boundaries and the shell is hence written as

$$P(\vec{R}_{obs}|\vec{R}_{sp}) = G(\vec{R}_{obs}|\vec{R}_{sp}) + P_{scat}(\vec{R}_{obs}|\vec{R}_{sp})$$

where the contribution of the scattering from the shell, P_{scat}, is written as

$$P_{scat}(\vec{R}_{obs}|\vec{R}_{sp}) = \frac{i}{4} e^{i\pi/4} \sum_{j=1}^{\infty} C_j \phi_j(z_{obs}) \left[\sum_{n=1}^{N} P_n(\vec{R}_{sp}) Q_{pjn}(\vec{R}_{obs}) + i\omega \sum_{n=1}^{N} \rho_n V_n(\vec{R}_{sp}) Q_{vjn}(\vec{R}_{obs}) \right] \ .$$

The order of summation (in *n* and *j*) has been written arbitrarily in the foregoing equation. An issue that must be resolved in the course of the study is the determination of which order of summation is more computationally efficient.

The quadratures can, in turn, be represented as weighted sums of values of the integrands, since a Gaussian quadrature procedure will be used. The terms can hence be rewritten as

$$\begin{aligned} Q_{vjn} &= \int_{S_n} \sqrt{\frac{2}{\pi(r_{obs-sh}\sqrt{k_0^2 - \lambda_j})}} e^{-i(r_{obs-sh}\sqrt{k_0^2-\lambda_j})} \phi_j(z_{sh}) dS \\ &= \sum^{M_n} W_{nm} f_{rjnm} f_{zjnm} \ , \end{aligned}$$

where W_{nm} is a set of Gaussian quadrature weights, and where

$$f_{rjnm} = \sqrt{\frac{2}{\pi(r_{obs-sh}\sqrt{k_0^2 - \lambda_j})}} e^{-i(r_{obs-sh}\sqrt{k_0^2-\lambda_j})} \ ,$$

and

$$f_{zjnm} = \phi_j(z_{sh}) \ .$$

For the sake of simplicity, the obvious dependence of r_{obs-sh} and z_{sh} on the indices *m* and *n* has been suppressed. Similarly, one has that

$$\begin{aligned} Q_{pjn} &= \int_{S_n} e^{-i(r_{obs-sh}\sqrt{k_0^2-\lambda_j})} \sqrt{\frac{2}{\pi(r_{obs-sh}\sqrt{k_0^2-\lambda_j})}} \\ &\quad [-i\sqrt{k_0^2-\lambda_j}\phi_j(z_{sh})\alpha_r + \phi_j'(z_{sh})\alpha_z]dS \\ &= \sum_{j=1}^{M_n} W_{nm} f_{rjnm} f_{rzjnm} \ , \end{aligned}$$

where

$$f_{rzjnm} = -i\sqrt{k_0^2-\lambda_j}\phi_j(z_{sh})\alpha_r + \phi_j'(z_{sh})\alpha_z \ .$$

A.8 PEKERIS WAVEGUIDE

In the case of this environment, a surface liquid layer of depth h lies over a liquid half-space having different acoustic properties. The specific form of the sound speed profile chosen as a function of depth, *z*, is

$$k^2(z_{fg}) = \begin{cases} \omega^2/c_1^2 & \text{,if } 0 \le z \le h \\ \omega^2/c_2^2 & \text{,if } h < z \end{cases} \ .$$

The density is also nonuniform, i.e.,

$$\rho(z_{fg}) = \begin{cases} \rho_1 & \text{if } 0 \le z \le h \\ \rho_2 & \text{if } h < z \end{cases} \ .$$

In the upper layer (i.e., for $0 \le z \le h$), the pressure field can be written in terms of the sum of a residue series and a branch line integral. In the present study, the branch line integral is ignored and the field is approximated as the sum of the terms of the residue series. The explicit form of the series is given as

$$G(\vec{R}_{fg}|\vec{R}_{sg}) = \frac{-i}{2h}\sum_{j=1}^{\infty} \frac{\sin\alpha_j z_{sg} \sin\alpha_j z_{fg} H_0^{(2)}(r\sqrt{k_1^2-\alpha_j^2})}{1 - \frac{1}{h}b^2 \frac{k_1^2(1-n^2)}{\alpha_j}\frac{1}{\alpha_j^2}\sin^2\alpha_j h \tan\alpha_j h} \ ,$$

where

$$b = \frac{\rho_1}{\rho_2}, \ k_1 = \frac{\omega}{c_1}, \ k_2 = \frac{\omega}{c_2}, \ n = \frac{c_1}{c_2},$$

and where the terms $\lambda_j = \alpha_j^2$ are poles of *G* which are located at values satisfying the dispersion relation

$$\tan(\alpha h) = -\frac{\alpha h}{b\sqrt{h^2k_1^2(1-n^2) - (\alpha h)^2}} \ .$$

In the foregoing equations, the subscript $_1$ refers to the properties of the upper layer and the subscript $_2$ refers to the properties of the lower layer. The term k_1 is the reference wave number mentioned previously, i.e., $k_1 = k_0$. Furthermore, only the real solutions of the dispersion relation are to be considered in the present instance. The complex solutions will correspond to nonpropagating modes which decay exponentially.

In the nomenclature developed in the foregoing sections, one has that

$$\phi_j(z) = \frac{-1}{\alpha_j} \sin(\alpha_j z) \ ,$$

The foregoing mode shape can be cast into a form that is particularly useful for interpreting the inter-modal target strengths defined previously. Specifically, note that

$$\phi_j(z) = \frac{-1}{2i\alpha_j} \left[e^{i(\alpha_j z)} - e^{-i(\alpha_j z)} \right] \ .$$

The partial source strength used for the calculation of D in equation (A.12) is thus

$$e^{-i\left(\frac{\vec{r}_{srf}\cdot\vec{r}_{0\ inc}}{r_{0\ inc}}\sqrt{k_0^2-\lambda_j}\right)}\phi_j(z_{srf}) =$$
$$\frac{-1}{2i\sqrt{\lambda_j}}\left[e^{i\left(\sqrt{\lambda_j}\vec{r}_{srf}\cdot\vec{e}_z-\frac{\vec{r}_{srf}\cdot\vec{r}_{0\ inc}}{r_{0\ inc}}\sqrt{k_0^2-\lambda_j}\right)} - e^{-i\left(\sqrt{\lambda_j}\vec{r}_{srf}\cdot\vec{e}_z+\frac{\vec{r}_{srf}\cdot\vec{r}_{0\ inc}}{r_{0\ inc}}\sqrt{k_0^2-\lambda_j}\right)}\right] \ ,$$

where use has been made of the relationship

$$z_{srf} = \vec{r}_{srf} \cdot \vec{e}_z \ .$$

This result is equivalent to having the target ensonified by two free field waves, one of which is traveling in an upward direction and the other of which is traveling in a downward direction. The depression/elevation angle, $\theta_{depression/elevation}$ is given by the expression

$$\cos(\theta_{depression/elevation}) = \sqrt{1 - \lambda_j / k_0^2} \ .$$

A.10 COORDINATE SYSTEM COORDINATION

The formulations of the propagation and structural problems each lend themselves to expression in a particular coordinate system. The systems are cylindrical, in the case of the propagation problem, with the origin lying at the surface of the water and Cartesian, in the case of the structural problem, with the origin lying somewhere inside of, or on, the surface of the shell. The cartesian coordinates to which reference is made for the structural problem are called, in the current CHIEF/MARTSAM usage, “global coordinates.” This distinguishes them from the “local coordiantes,” which are used in the individual finite elements. The assumption is made that the x_1 axis lies along the axis of symmetry of the body being considered. The x_2 and x_3 axes are chosen such that x_3 points in the vertical downward direction, x_2 lies in the horizontal plane, and the set forms a right-handed triad. In the case of the cylindrical system, the z coordinate (depth) is taken to be a translated version of x_3 in the Cartesian system. The radial variable in the cylindrical system is given by the expression

$$r = \sqrt{x_1^2 + x_2^2} \ .$$

An aximuthal angle variable ϕ_a is needed to specify the aspect of the shell relative to the field point location (source or receiver). The convention chosen is the one currently used by the CHIEF/MARTSAM software to specify target aspect relative to an incident plane wave. A second angle (elevation) is ignored in this study since it is not particularly useful in the context of a refractive environment.

Given the cartesian coordinates (x_1, x_2, x_3) of a point on the wetted surface of the shell, then the cylindrical coordinates of that point (relative to the field point) are given as

$$\begin{aligned} r &= \sqrt{(x_1 - r_0 \cos\phi_{a0})^2 + (x_2 - r_0 \sin\phi_{a0})^2} \\ z &= z_0 + x_3 \ , \end{aligned}$$

where r_0 is the cylindrical range from the field point to the origin of the Cartesian system, z_0 is the depth (in the cylindrical system) of the origin of the Cartesian system, and ϕ_{a0} is the aspect of the target relative to the line joining the field point and the x_1 axis of the cartesian coordinate system. In previous sections (A.8 and A.9), it is equation (A.14) that is used to calculate coordinates for use in the generation of coefficients for use in equation (A.6) and equation (A.13).

A.11 APPROXIMATIONS IN SURFACE PRESSURES AND VELOCITIES

A particular approximation is used in the calculation of the surface pressures and velocities that is justified in the particular cases that will be of interest in the present study. The residue series representation of the propagation Green's function has regions in depth and range for which it does not converge. While these regions are not important from the standpoint of the calculation of the incident pressure from a distant source and the far-field scattered pressures, they are important from the standpoint of the solution of the integral equation defining the surface pressures and velocities on the excited shell. It was deemed reasonable to use the free-field propagation Green's function in the calculations involved in solving the integral equation. The heuristic justification derives from the notion that the distances between points on the shell are much smaller than their distances from corresponding points on the image shell, and also from the notion that refractive effects at these distances will be relatively small. This approximation can also be cast into the form of a low-order term in a proposed sequence of approximations to the actual solution. This sequence is developed in the following analysis. Write the differential equation for the Green's function in the form

$$\mathcal{L}(G) = \delta - \delta_- \ ,$$

where the differential operator $\mathcal{L}$ represents the wave equation in a refractive environment that includes not only the half-space in question, but also for an image half-space above, i.e., the composite medium has a sound speed profile that is symmetric in depth about the depth origin in the actual medium. In addition, the terms δ and δ_- represent sources at the actual source point

and at the image source point above the surface, respectively. The change in sign for the image point presence of a pressure release boundary as opposed to a rigid boundary.

The foregoing equation can be rewritten in terms of a wave operator for a uniform medium and a residual operator embodying the depth-dependent speed of sound. The result is

$$(\mathcal{L}_0 + \delta\mathcal{L})G = \delta - \delta_- \quad ,$$

where $\mathcal{L}_0$ is a differential operator for an approximate uniform medium, and $\delta\mathcal{L}$ embodies the refractive effects of the nonuniform sound speed profile. This equation is written in a somewhat more convenient form as

$$\mathcal{L}_0 G = \delta - \delta_- - \delta\mathcal{L}G \quad .$$

Using the inverse operator, G_0, one has the result that

$$G_0 \circ \mathcal{L}_0 G = G_0 \circ \delta - G_0 \circ \delta_- - G_0 \circ \delta\mathcal{L}G \ ,$$

where the implied integration is over the entire domain of definition of G and $\mathcal{L}$.

From the definition of G_0, one has the problem cast into the following integral equation:

$$G = G_0 - G_{0-} - G_0 \circ \delta\mathcal{L}G. \tag{A.15}$$

The problem of solving for the Green's function is hence cast into the form of solving the foregoing problem. Under certain circumstances, the problem can be solved by the method of Picard iteration. Hence, one generates a sequence of approximations, $G_{[n]}$, to the function G with the hope that the sequence converges to the desired function. Specifically, one starts with G_0 and $G_{0\_}$ and one constructs the sequence

$$\begin{aligned}
G_{[1]} &= G_0 - G_{0-} - G_0 \circ \delta\mathcal{L}G_0 \\
G_{[2]} &= G_0 - G_{0-} - G_0 \circ \delta\mathcal{L}G_{[1]} \\
&\vdots \quad\quad \vdots \\
G_{[n+1]} &= G_0 - G_{0-} - G_0 \circ \delta\mathcal{L}G_{[n]} \\
&\vdots \quad\quad \vdots
\end{aligned}$$

This sequence of approximations to the Green's function will, under certain circumstances (unknown at this point), converge. It will, for no particularly good reason, be assumed to converge. In this context, the approach to be used in the current study can be thought of as the 0-th order approximation. While the higher order approximations have not been used in this study, the value of this formulation is that it provides a constructive approach for calculating each term of the sequence.

A variant of the lowest order approximation which is of particular interest is

$$G_{[0']}(\vec{R}_{obs}|\vec{R}_{sp}) = G_0 - G_{0-}.$$

This approximation will capture important multiple scattering effects for a target near the pressure release boundary.

A.12 APPROXIMATE MULTIPLE SCATTERING GREEN'S FUNCTION FOR SURFACE INTEGRAL EQUATION

The Surface Integral Equation calls for the use of the full refractive Green's function for use in the kernel. Difficulties with a convenient representation suggest the use of simpler, approximate forms. A method for partially implementing the approximate scheme in the previous section is detailed here.

Let the vectors $\vec{R}_{fp}$ and $\vec{R}_{sp}$ be the field and source points for the Green's function in the following free-space boundary value problem

$$(\nabla^2_{R_{fp}} + k_0^2) G_0(\vec{R}_{fp}|\vec{R}_{sp}) = 0 \text{ in } V \ ,$$

and

$$\lim_{r_p \to \infty} r_p |\frac{\partial G_0}{\partial r} + ik_0 G_0| = 0 \ ,$$

where $\tau_p = |\vec{R}_{fp} - \vec{R}_{sp}|, k_0 = \omega / c_0$.

In the present example, let $\vec{R}_{fp} = \vec{R}_{fg} = \vec{R}_f$. We then have the result

$$G_0(\vec{R}_f|\vec{R}_{sp})(\nabla^2_{R_f} + k^2(z_f))G(\vec{R}_f|\vec{R}_{sg}) - G(\vec{R}_f|\vec{R}_{sg})(\nabla^2_{R_f} + k_0^2)G_0(\vec{R}_f|\vec{R}_{sp}) = 0 \ ,$$

or

$$\begin{aligned} G_0(\vec{R}_f|\vec{R}_{sp})\nabla^2_{R_f} G(\vec{R}_f|\vec{R}_{sg}) \ - \ & G(\vec{R}_f|\vec{R}_{sg})\nabla^2_{R_f} G_0(\vec{R}_f|\vec{R}_{sp}) + \\ & (k^2(z_f) - k_0^2) G_0(\vec{R}_f|\vec{R}_{sp}) G(\vec{R}_f|\vec{R}_{sg}) = 0 \ . \end{aligned} \tag{A.17}$$

The following identities are useful in simplifying the foregoing expression:

$$\begin{aligned} \nabla_{R_f} \cdot [G_0(\vec{R}_f|\vec{R}_{sp})\nabla_{R_f} G(\vec{R}_f|\vec{R}_{sg})] = \ & \nabla_{R_f} G_0(\vec{R}_f|\vec{R}_{sp}) \cdot \nabla_{R_f} G(\vec{R}_f|\vec{R}_{sg}) + \\ & G_0(\vec{R}_f|\vec{R}_{sp})\nabla^2_{R_f} G(\vec{R}_f|\vec{R}_{sg}) = 0 \ , \end{aligned}$$

and

$$\begin{aligned} \nabla_{R_f} \cdot [G(\vec{R}_f|\vec{R}_{sg})\nabla_{R_f} G_0(\vec{R}_f|\vec{R}_{sp})] \ = \ & \nabla_{R_f} G(\vec{R}_f|\vec{R}_{sg}) \cdot \nabla_{R_f} G_0(\vec{R}_f|\vec{R}_{sp}) + \\ & G(\vec{R}_f|\vec{R}_{sg})\nabla^2_{R_f} G_0(\vec{R}_f|\vec{R}_{sp}) = 0 \ . \end{aligned}$$

Hence, we can reqrite equation (A.17) in a simplified form as

$$\begin{aligned} \nabla_{R_f} \cdot [G_0(\vec{R}_f|\vec{R}_{sp})\nabla_{R_f} G(\vec{R}_f|\vec{R}_{sg}) \ - \ & G(\vec{R}_f|\vec{R}_{sg})\nabla_{R_f} G_0(\vec{R}_f|\vec{R}_{sp})] + \\ & (k^2(z_f) - k_0^2) G_0(\vec{R}_f|\vec{R}_{sp}) G(\vec{R}_f|\vec{R}_{sg}) = 0. \end{aligned}$$

A variant of the lowest order approximation which is of particular interest is

$$\int_{V-V_{\epsilon g}-V_{\epsilon p}} \Big\{\nabla_{R_f}\cdot[G_0(\vec{R}_f|\vec{R}_{sp})\nabla_{R_f}G(\vec{R}_f|\vec{R}_{sg})- G(\vec{R}_f|\vec{R}_{sg})\nabla_{R_f}G_0(\vec{R}_f|\vec{R}_{sp})] + [k^2(z_f)-k_0^2]G_0(\vec{R}_f|\vec{R}_{sp})G(\vec{R}_f|\vec{R}_{sg})\Big\}\,dV = 0.$$

This is readily converted into a surface integral of the form

$$\begin{aligned}\int_{S_{\epsilon g}+S_{\epsilon p}+S_{UPPER}+S_{LOWER}} & [G_0(\vec{R}_f|\vec{R}_{sp})\nabla_{R_f}G(\vec{R}_f|\vec{R}_{sg}) - G(\vec{R}_f|\vec{R}_{sg})\nabla_{R_f}G_0(\vec{R}_f|\vec{R}_{sp})]\cdot\vec{n}_{fl}dS \\ + \int_{V-V_{\epsilon g}-V_{\epsilon p}} & [k^2(z_f)-k_0^2]G_0(\vec{R}_f|\vec{R}_{sp})G(\vec{R}_f|\vec{R}_{sg})dV = 0\ ,\end{aligned} \tag{A.18}$$

where $\vec{n}_{fl}$ is the outward unit normal to the fluid.

The integrals over the surfaces S_{eg} and S_{ep} have been particularly simple limiting forms. Note that

$$\begin{aligned}\int_{S_{\epsilon g}} G_0(\vec{R}_f|\vec{R}_{sp})\nabla_{R_f}G(\vec{R}_f|\vec{R}_{sg})\cdot\vec{n}_{fl}dS &\doteq G_0(\vec{R}_{sg}|\vec{R}_{sp})\int_{S_{\epsilon g}}\nabla_{R_f}G(\vec{R}_f|\vec{R}_{sg})\cdot\vec{n}_{fl}dS \\ &\doteq G_0(\vec{R}_{sg}|\vec{R}_{sp})\left[-(4\pi\epsilon^2)\frac{\partial}{\partial\epsilon}\left(\frac{e^{-ik\epsilon}}{4\pi\epsilon}\right)\right] \\ &\doteq G_0(\vec{R}_{sg}|\vec{R}_{sp})\left[-(4\pi\epsilon^2)\left(-ik\frac{e^{-ik\epsilon}}{4\pi\epsilon}-\frac{e^{-ik\epsilon}}{4\pi\epsilon^2}\right)\right] \\ &\doteq G_0(\vec{R}_{sg}|\vec{R}_{sp})\ .\end{aligned}$$

Similarly, one has

$$\begin{aligned}\int_{S_{\epsilon p}} G(\vec{R}_f|\vec{R}_{sg})\nabla_{R_f}G_0(\vec{R}_f|\vec{R}_{sp})\cdot\vec{n}_{fl}dS &\doteq G(\vec{R}_{sp}|\vec{R}_{sg})\int_{S_{\epsilon p}}\nabla_{R_f}G_0(\vec{R}_f|\vec{R}_{sp})\cdot\vec{n}_{fl}dS \\ &\doteq G(\vec{R}_{sp}|\vec{R}_{sg})\left[-(4\pi\epsilon^2)\frac{\partial}{\partial\epsilon}(\frac{e^{-ik\epsilon}}{4\pi\epsilon})\right] \\ &\doteq G(\vec{R}_{sp}|\vec{R}_{sg})\left[-(4\pi\epsilon^2)\left(-ik\frac{e^{-ik\epsilon}}{4\pi\epsilon}-\frac{e^{-ik\epsilon}}{4\pi\epsilon^2}\right)\right] \\ &\doteq G(\vec{R}_{sp}|\vec{R}_{sg})\ .\end{aligned}$$

Note also that

$$\begin{aligned}\int_{S_{\epsilon g}} G(\vec{R}_f|\vec{R}_{sg}))\nabla_{R_f}G_0(\vec{R}_f|\vec{R}_{sp})\cdot\vec{n}_{fl}dS &\doteq |\nabla_{R_f}G_0(\vec{R}_{sg}|\vec{R}_{sp})|\int_{S_{\epsilon p}}G(\vec{R}_f|\vec{R}_{sg})\vec{e}\cdot\vec{n}_{fl}dS \\ &\doteq |\nabla_{R_f}G_0(\vec{R}_{sg}|\vec{R}_{sp})|\frac{1}{4\pi\epsilon}\int_{S_{\epsilon p}}\vec{e}\cdot\vec{n}_{fl}dS \\ &\doteq 0.\end{aligned}$$

Similarly, one has

$$\begin{aligned}\int_{S_{\epsilon p}} G_0(\vec{R}_f|\vec{R}_{sp}))\nabla_{R_f} G(\vec{R}_f|\vec{R}_{sg})\cdot\vec{n}_{fl}dS &\doteq |\nabla_{R_f} G(\vec{R}_{sp}|\vec{R}_{sg})|\int_{S_{\epsilon g}} G_0(\vec{R}_f|\vec{R}_{sp})\vec{e}\cdot\vec{n}_{fl}dS \\ &\doteq |\nabla_{R_f} G(\vec{R}_{sp}|\vec{R}_{sg})|\frac{1}{4\pi\epsilon}\int_{S_{\epsilon g}}\vec{e}\cdot\vec{n}_{fl}dS \\ &\doteq 0.\end{aligned}$$

These four approximations are exact in the limit as ε shrinks to 0. The surface integral can thus be written as

$$\begin{aligned}&G_0(\vec{R}_{sg}|\vec{R}_{sp}) - G(\vec{R}_{sp}|\vec{R}_{sg}) + \\ &\quad\int_{S_{UPPER}}[G_0(\vec{R}_{UPPER}|\vec{R}_{sp})\nabla_{R_{UPPER}}G(\vec{R}_{UPPER}|\vec{R}_{sg}) - \\ &\quad G(\vec{R}_{UPPER}|\vec{R}_{sg})\nabla_{R_{UPPER}}G_0(\vec{R}_{UPPER}|\vec{R}_{sp})]\cdot\vec{n}_{fl}dS + \\ &\quad\int_{S_{LOWER}}[G_0(\vec{R}_{LOWER}|\vec{R}_{sp})\nabla_{R_{LOWER}}G(\vec{R}_{LOWER}|\vec{R}_{sg}) - \\ &\quad G(\vec{R}_{LOWER}|\vec{R}_{sg})\nabla_{R_{LOWER}}G_0(\vec{R}_{LOWER}|\vec{R}_{sp})]\cdot\vec{n}_{fl}dS = 0.\end{aligned} \tag{A.19}$$

The surface integral can thus be rewritten as

$$\begin{aligned}&G_0(\vec{R}_{sg}|\vec{R}_{sp}) = G(\vec{R}_{sp}|\vec{R}_{sg}) - \\ &\quad\int_{S_{UPPER}}[G_0(\vec{R}_{UPPER}|\vec{R}_{sp})\nabla_{R_{UPPER}}G(\vec{R}_{UPPER}|\vec{R}_{sg}) - \\ &\quad G(\vec{R}_{UPPER}|\vec{R}_{sg})\nabla_{R_{UPPER}}G_0(\vec{R}_{UPPER}|\vec{R}_{sp})]\cdot\vec{n}_{fl}dS \\ &\quad -\int_{S_{LOWER}}[G_0(\vec{R}_{LOWER}|\vec{R}_{sp})\nabla_{R_{LOWER}}G(\vec{R}_{LOWER}|\vec{R}_{sg}) - \\ &\quad G(\vec{R}_{LOWER}|\vec{R}_{sg})\nabla_{R_{LOWER}}G_0(\vec{R}_{LOWER}|\vec{R}_{sp})]\cdot\vec{n}_{fl}dS.\end{aligned} \tag{A.20}$$

A change of notation can be invoked, and the symmetry of the Green's function can be used to cast the problem into a form familiar to those working in scattering theory

$$\begin{aligned}&G_0(\vec{R}_{obs}|\vec{R}_{sp}) = G(\vec{R}_{obs}|\vec{R}_{sp}) - \\ &\quad\int_{S_{UPPER}}[G_0(\vec{R}_{UPPER}|\vec{R}_{sp})\nabla_{R_{UPPER}}G(\vec{R}_{obs}|\vec{R}_{UPPER}) - \\ &\quad G(\vec{R}_{obs}|\vec{R}_{UPPER})\nabla_{R_{UPPER}}G_0(\vec{R}_{UPPER}|\vec{R}_{sp})]\cdot\vec{n}_{fl}dS \\ &\quad -\int_{S_{LOWER}}[G_0(\vec{R}_{LOWER}|\vec{R}_{sp})\nabla_{R_{LOWER}}G(\vec{R}_{obs}|\vec{R}_{LOWER}) - \\ &\quad G(\vec{R}_{obs}|\vec{R}_{LOWER})\nabla_{R_{LOWER}}G_0(\vec{R}_{LOWER}|\vec{R}_{sp})]\cdot\vec{n}_{fl}dS \\ &\quad +\int_V (k^2(z_f) - k_0^2)G_0(\vec{R}_f|\vec{R}_{sp})G(\vec{R}_f|\vec{R}_{sg})dV\ ,\end{aligned}$$

where R_{obs} is substituted for the term R_{sg}.

$$
\begin{aligned}
G_0(\vec{R}_{obs}|\vec{R}_{sp}) = G(\vec{R}_{obs}|\vec{R}_{sp}) - \\
\int_{S_{UPPER}} [G_0(\vec{R}_{UPPER}|\vec{R}_{sp}) \nabla_{R_{UPPER}} G(\vec{R}_{obs}|\vec{R}_{UPPER})] \cdot \vec{n}_{fl} dS \\
+ \int_{S_{LOWER}} [\nabla_{R_{LOWER}} G_0(\vec{R}_{LOWER}|\vec{R}_{sp}) G(\vec{R}_{obs}|\vec{R}_{LOWER})] \cdot \vec{n}_{fl} dS \\
+ \int_V (k^2(z_f) - k_0^2) G_0(\vec{R}_f|\vec{R}_{sp}) G(\vec{R}_f|\vec{R}_{sg}) dV
\end{aligned}
$$

or

$$
\begin{aligned}
G(\vec{R}_{obs}|\vec{R}_{sp}) = G_0(\vec{R}_{obs}|\vec{R}_{sp}) + \\
\int_{S_{UPPER}} [G_0(\vec{R}_{UPPER}|\vec{R}_{sp}) \nabla_{R_{UPPER}} G(\vec{R}_{obs}|\vec{R}_{UPPER})] \cdot \vec{n}_{fl} dS \\
- \int_{S_{LOWER}} [\nabla_{R_{LOWER}} G_0(\vec{R}_{LOWER}|\vec{R}_{sp}) G(\vec{R}_{obs}|\vec{R}_{LOWER})] \cdot \vec{n}_{fl} dS \\
- \int_V (k^2(z_f) - k_0^2) G_0(\vec{R}_f|\vec{R}_{sp}) G(\vec{R}_f|\vec{R}_{sg}) dV \ .
\end{aligned}
\tag{A.21}
$$

Consider the special case of a uniform environment with a pressure release upper surface and a rigid lower surface. The foregoing equation thus becomes

$$
\begin{aligned}
G_0(\vec{R}_{obs}|\vec{R}_{sp}) = G(\vec{R}_{obs}|\vec{R}_{sp}) - \\
\int_{S_{UPPER}} [G_0(\vec{R}_{UPPER}|\vec{R}_{sp}) \nabla_{R_{fl}} G(\vec{R}_{obs}|\vec{R}_{UPPER})] \cdot \vec{n}_{UPPER} dS \\
+ \int_{S_{LOWER}} [\nabla_{R_{fl}} G_0(\vec{R}_{LOWER}|\vec{R}_{sp}) G(\vec{R}_{obs}|\vec{R}_{LOWER})] \cdot \vec{n}_{LOWER} dS.
\end{aligned}
$$

This equation can also be written in terms of image sources as follows

$$
G_0(\vec{R}_{obs}|\vec{R}_{sp}) \doteq G(\vec{R}_{obs}|\vec{R}_{sp}) + G_0(\vec{R}_{obs}|\vec{R}_{sp\ upper\ image}) - G_0(\vec{R}_{obs}|\vec{R}_{sp\ lower\ image}) \ , \tag{A.22}
$$

where $\vec{R}_{sp\ image}$ is the location of the image of the source point above the pressure release surface.

A special set of coordinates will be chosen with the origin at the phase center of the target. The pressure release surface will have a *z*-coordinate of z_{UPPER} and the lower rigid boundary will have a *z*-coordinate of z_{LOWER}. Using equation (A.22), the Green's function (equation A.21) is hence written approximately as follows

$$
\begin{aligned}
G_{[0']}(\vec{R}_{obs}|\vec{R}_{sp}) = \frac{e^{-ik|R_{obs}-R_{sp}|}}{4\pi|\vec{R}_{obs}-\vec{R}_{sp}|} - \frac{e^{-ik|R_{obs}-R_{sp\ upper\ image}|}}{4\pi|\vec{R}_{obs}-\vec{R}_{sp\ upper\ image}|} + \\
\frac{e^{-ik|\vec{R}_{obs}-\vec{R}_{sp\ lower\ image}|}}{4\pi|\vec{R}_{obs}-\vec{R}_{sp\ lower\ image}|} \ ,
\end{aligned}
\tag{A.23}
$$

where

$$|\vec{R}_{obs} - \vec{R}_{sp}| = \sqrt{(x_{obs} - x_{sp})^2 + (y_{obs} - y_{sp})^2 + (z_{obs} - z_{sp})^2} \ ,$$

$$|\vec{R}_{obs} - \vec{R}_{sp\ upper\ image}| = \sqrt{(x_{obs} - x_{sp})^2 + (y_{obs} - y_{sp})^2 + (z_{obs} - (2z_{UPPER} - z_{sp}))^2} \ ,$$

and

$$|\vec{R}_{obs} - \vec{R}_{sp\ lower\ image}| = \sqrt{(x_{obs} - x_{sp})^2 + (y_{obs} - y_{sp})^2 + (z_{obs} - (2z_{LOWER} - z_{sp}))^2} \ .$$

It is equation (A.23), which is an implementation of equation (A.16), that is used in place of G_0 in the Surface Integral Equation (A.6).

An alternative, which is valid only for the approximation $G_{[0']}(\vec{R}_{obs}|\vec{R}_{sp}$, is to use an image target with the pressure and velocities being of opposite sign to those of the true target. Equation (A.6) can be manipulated as follows to yield a form that is particularly easy to implement:

$$\frac{1}{2}P(\vec{R}_{sg}|\vec{R}_{sp}) = G(\vec{R}_{sp}|\vec{R}_{sg}) + \int_{S_{sh}} [P(\vec{R}_{sh}|\vec{R}_{sp})\nabla_{R_{sh}} G_{[0']}(\vec{R}_{sh}|\vec{R}_{sg}) - G_{[0']}(\vec{R}_{sh}|\vec{R}_{sg})\nabla_{R_{sh}} P(\vec{R}_{sh}|\vec{R}_{sp})] \cdot \vec{n}_{sh} dS \ ,$$

or

$$\frac{1}{2}P(\vec{R}_{sg}|\vec{R}_{sp}) = G_+(\vec{R}_{sp}|\vec{R}_{sg}) - G_-(\vec{R}_{sp\ image}|\vec{R}_{sg}) + \int_{S_{sh}} [P(\vec{R}_{sh}|\vec{R}_{sp})\nabla_{R_{sh}} G_0(\vec{R}_{sh}|\vec{R}_{sg}) - G_0(\vec{R}_{sh}|\vec{R}_{sg})\nabla_{R_{sh}} P(\vec{R}_{sh}|\vec{R}_{sp})] \cdot \vec{n}_{sh} dS - \int_{S_{sh\ image}} [P(\vec{R}_{sh}|\vec{R}_{sp})\nabla_{R_{sh}} G_0(\vec{R}_{sh}|\vec{R}_{sg}) - G_0(\vec{R}_{sh}|\vec{R}_{sg})\nabla_{R_{sh}} P(\vec{R}_{sh}|\vec{R}_{sp})] \cdot \vec{n}_{sh} dS \ ,$$

where the functions $G_+(\vec{R}_{sp}|\vec{R}_{sg}$ and $G_-(\vec{R}_{sp\ image}|\vec{R}_{sg}$ are the source terms (Green's functions) for the environments which have the sound speed profile reflected up above the pressure release surface, i.e., a mirror image environment lying above the surface.

The specific computer implementation would be as follows. Solve two separate problems and add the solutions:

$$P(\vec{R}_{sg}|\vec{R}_{sp}) = P_+(\vec{R}_{sg}|\vec{R}_{sp}) - P_-(\vec{R}_{sg}|\vec{R}_{sp}) \ ,$$

where

$$\frac{1}{2}P_+(\vec{R}_{sg}|\vec{R}_{sp}) = G_+(\vec{R}_{sp}|\vec{R}_{sg}) + \int_{S_{sh}} [P_+(\vec{R}_{sh}|\vec{R}_{sp})\nabla_{R_{sh}} G_0(\vec{R}_{sh}|\vec{R}_{sg}) - G_0(\vec{R}_{sh}|\vec{R}_{sg})\nabla_{R_{sh}} P_+(\vec{R}_{sh}|\vec{R}_{sp})] \cdot \vec{n}_{sh} dS - \int_{S_{sh\ image}} [P_+(\vec{R}_{sh}|\vec{R}_{sp})\nabla_{R_{sh}} G_0(\vec{R}_{sh}|\vec{R}_{sg}) - G_0(\vec{R}_{sh}|\vec{R}_{sg})\nabla_{R_{sh}} P_+(\vec{R}_{sh}|\vec{R}_{sp})] \cdot \vec{n}_{sh} dS$$

and

$$\frac{1}{2}P_-(\vec{R}_{sg}|\vec{R}_{sp}) = G_-(\vec{R}_{sp\ image}|\vec{R}_{sg}) + \int_{S_{sh}} [P_-(\vec{R}_{sh}|\vec{R}_{sp})\nabla_{R_{sh}}G_0(\vec{R}_{sh}|\vec{R}_{sg}) - G_0(\vec{R}_{sh}|\vec{R}_{sg})\nabla_{R_{sh}}P_-(\vec{R}_{sh}|\vec{R}_{sp})] \cdot \vec{n}_{sh}dS - \int_{S_{sh\ image}} [P_-(\vec{R}_{sh}|\vec{R}_{sp})\nabla_{R_{sh}}G_0(\vec{R}_{sh}|\vec{R}_{sg}) - G_0(\vec{R}_{sh}|\vec{R}_{sg})\nabla_{R_{sh}}P_-(\vec{R}_{sh}|\vec{R}_{sp})] \cdot \vec{n}_{sh}dS \ .$$

A separate target must be placed at the target image location, and the appropriate change in sign must be made in its contributions to the integral equation. It may require reprogramming the integral equation solver in CHIEF to put in this change of sign. Since the "imaging" effect is only due to the particular representation used for the propagation Green's function, no software changes should be needed with respect to the usage of the elastic target effects. Note that the driving functions for the equations, $G_+(\vec{R}_{sp}|\vec{R}_{sg}$ and $G_-(\vec{R}_{sp\ image}|\vec{R}_{sg}$, are Green's functions for the reflected environment, rather than for the original half space; thus, care must be taken to use the original modes correctly when the target and source are not in the same half-space.

From symmetry considerations, one has that

$$P_+(\vec{R}_{sg}|\vec{R}_{sp}) = -P_-(\vec{R}_{sg\ image}|\vec{R}_{sp}) \ .$$

This means that one need only solve one of the two foregoing integral equations and then correctly combine the solution for the true target with the solution at the appropriate image points of the image target in order to get the full solution.

A.13 SPECIAL PARTIAL SUMS OF INTEREST

Equation (A.22) can be rewritten, for the case wherein the effect of the upper surface is to be neglected, as follows:

$$G(\vec{R}_{obs}|\vec{R}_{sp}) = G_0(\vec{R}_{obs}|\vec{R}_{sp}) - \int_{S_{LOWER}} [\nabla_{R_{fl}}G_0(\vec{R}_{LOWER}|\vec{R}_{sp})G(\vec{R}_{obs}|\vec{R}_{LOWER})] \cdot \vec{n}_{LOWER}dS.$$

Note that the equation has now been cast into the form of a fixed point problem. In the event that the right-hand side is a contraction mapping and that one can locate a starting point in the domain of attraction of the fixed point, then a candidate solution technique is Picard iteration. In particular, the problem then becomes equivalent to the following sequence of problems:

$$G^{[1]}(\vec{R}_{obs}|\vec{R}_{sp}) = G_0(\vec{R}_{obs}|\vec{R}_{sp}) - \int_{S_{LOWER}} [\nabla_{R_{fl}}G_0(\vec{R}_{LOWER}|\vec{R}_{sp})G_0(\vec{R}_{obs}|\vec{R}_{LOWER})] \cdot \vec{n}_{LOWER}dS \ ,$$

and

$$G^{[2]}(\vec{R}_{obs}|\vec{R}_{sp}) = G_0(\vec{R}_{obs}|\vec{R}_{sp}) - \int_{S_{LOWER}} [\nabla_{R_{fl}}G_0(\vec{R}_{LOWER}|\vec{R}_{sp})G^{[1]}(\vec{R}_{obs}|\vec{R}_{LOWER})] \cdot \vec{n}_{LOWER}dS.$$

The n-th iteration is given by

$$G^{[n]}(\vec{R}_{obs}|\vec{R}_{sp}) = G_0(\vec{R}_{obs}|\vec{R}_{sp}) \\ - \int_{S_{LOWER}} [\nabla_{R_{fl}} G_0(\vec{R}_{LOWER}|\vec{R}_{sp}) G^{[n-1]}(\vec{R}_{obs}|\vec{R}_{LOWER})] \cdot \vec{n}_{LOWER} dS.$$

Use is to be made of equation (A.22), which can be rewritten (neglecting the upper surface) as

$$G(\vec{R}_{obs}|\vec{R}_{sp}) \doteq G_0(\vec{R}_{obs}|\vec{R}_{sp}) + G_0(\vec{R}_{obs}|\vec{R}_{sp\ lower\ image}) \ .$$

The foregoing equations yield the result

$$G(\vec{R}_{obs}|\vec{R}_{sp}) = G_0(\vec{R}_{obs}|\vec{R}_{sp}) \\ - \int_{S_{LOWER}} [\nabla_{R_{fl}} G_0(\vec{R}_{LOWER}|\vec{R}_{sp}) \left\{ G_0(\vec{R}_{obs}|\vec{R}_{LOWER}) + \right. \\ \left. G_0(\vec{R}_{obs\ image}|\vec{R}_{LOWER}) \right\}] \cdot \vec{n}_{LOWER} dS \ \ ,$$

so the first iterate is given as

$$G^{[1]}(\vec{R}_{obs}|\vec{R}_{sp}) = G_0(\vec{R}_{obs}|\vec{R}_{sp}) \\ - \int_{S_{LOWER}} [\nabla_{R_{fl}} G_0(\vec{R}_{LOWER}|\vec{R}_{sp}) G_0(\vec{R}_{obs}|\vec{R}_{LOWER})] \cdot \vec{n}_{LOWER} dS \\ = G_0(\vec{R}_{obs}|\vec{R}_{sp}) \\ -\frac{1}{2} \int_{S_{LOWER}} [\nabla_{R_{fl}} G_0(\vec{R}_{LOWER}|\vec{R}_{sp}) G(\vec{R}_{obs}|\vec{R}_{LOWER})] \cdot \vec{n}_{LOWER} dS \\ = G_0(\vec{R}_{obs}|\vec{R}_{sp}) + \frac{1}{2} G_0(\vec{R}_{obs\ lower\ image}|\vec{R}_{sp}) \ .$$

The second iterate is given by

$$G^{[2]}(\vec{R}_{obs}|\vec{R}_{sp}) = G_0(\vec{R}_{obs}|\vec{R}_{sp}) \\ - \int_{S_{LOWER}} [\nabla_{R_{fl}} G_0(\vec{R}_{LOWER}|\vec{R}_{sp}) G^{[1]}(\vec{R}_{obs}|\vec{R}_{LOWER})] \cdot \vec{n}_{LOWER} dS \\ = G_0(\vec{R}_{obs}|\vec{R}_{sp}) \\ - \int_{S_{LOWER}} [\nabla_{R_{fl}} G_0(\vec{R}_{LOWER}|\vec{R}_{sp}) G_0(\vec{R}_{obs}|\vec{R}_{sp}) + \frac{1}{2} G_0(\vec{R}_{obs\ lower\ im} \\ = G_0(\vec{R}_{obs}|\vec{R}_{sp}) + \frac{1}{2} G_0(\vec{R}_{obs\ lower\ image}|\vec{R}_{sp}) + \frac{1}{4} G_0(\vec{R}_{obs\ lower\ image}|$$

The n-th iterate has the simple form

$$G^{[n]}(\vec{R}_{obs}|\vec{R}_{sp}) = \left\{ \sum_{j=0}^{n} \frac{1}{2^j} \right\} G_0(\vec{R}_{obs\ lower\ image}|\vec{R}_{sp})$$

or

$$G^{[n]}(\vec{R}_{obs}|\vec{R}_{sp}) = \left\{ \sum_{j=0}^{n} \frac{1}{2^j} \right\} G_0(\vec{R}_{obs}|\vec{R}_{sp\ lower\ image}) \ .$$

Alternatively, equation (A.22) can be rewritten, for the case wherein the effect of the lower surface is to be neglected, as follows:

$$G(\vec{R}_{obs}|\vec{R}_{sp}) = G_0(\vec{R}_{obs}|\vec{R}_{sp}) + \int_{S_{UPPER}} [G_0(\vec{R}_{UPPER}|\vec{R}_{sp}) \nabla_{R_{fl}} G(\vec{R}_{obs}|\vec{R}_{UPPER})] \cdot \vec{n}_{UPPER} dS \ .$$

Note that the equation has now been cast into the form of a fixed point problem. In the event that the right-hand side is a contraction mapping, and one can locate a starting point in the domain of attraction of the fixed point, then a candidate solution technique is Picard iteration. In particular, the problem then becomes equivalent to the following sequence of problems:

$$G^{[1]}(\vec{R}_{obs}|\vec{R}_{sp}) = G_0(\vec{R}_{obs}|\vec{R}_{sp}) + \int_{S_{UPPER}} [G_0(\vec{R}_{UPPER}|\vec{R}_{sp}) \nabla_{R_{fl}} G_0(\vec{R}_{obs}|\vec{R}_{UPPER})] \cdot \vec{n}_{UPPER} dS \ ,$$

and

$$G^{[2]}(\vec{R}_{obs}|\vec{R}_{sp}) = G_0(\vec{R}_{obs}|\vec{R}_{sp}) + \int_{S_{UPPER}} [G_0(\vec{R}_{UPPER}|\vec{R}_{sp}) \nabla_{R_{fl}} G^{[1]}(\vec{R}_{obs}|\vec{R}_{UPPER})] \cdot \vec{n}_{UPPER} dS \ .$$

The n-th iteration is given by

$$G^{[n]}(\vec{R}_{obs}|\vec{R}_{sp}) = G_0(\vec{R}_{obs}|\vec{R}_{sp}) + \int_{S_{UPPER}} [G_0(\vec{R}_{UPPER}|\vec{R}_{sp}) \nabla_{R_{fl}} G^{[n-1]}(\vec{R}_{obs}|\vec{R}_{UPPER})] \cdot \vec{n}_{UPPER} dS \ .$$

Use is to be made of equation (A.22), which can be rewritten (neglecting the upper surface) as

$$G(\vec{R}_{obs}|\vec{R}_{sp}) \doteq G_0(\vec{R}_{obs}|\vec{R}_{sp}) - G_0(\vec{R}_{obs}|\vec{R}_{sp\ upper\ image}) \ .$$

The foregoing equations yield the result

$$\begin{aligned} G(\vec{R}_{obs}|\vec{R}_{sp}) &= G_0(\vec{R}_{obs}|\vec{R}_{sp}) \\ &+ \int_{S_{UPPER}} [\nabla_{R_{fl}} G_0(\vec{R}_{UPPER}|\vec{R}_{sp}) \left\{ G_0(\vec{R}_{obs}|\vec{R}_{UPPER}) - \right. \\ &\qquad \left. G_0(\vec{R}_{obs\ image}|\vec{R}_{UPPER}) \right\}] \cdot \vec{n}_{UPPER} dS \ , \end{aligned}$$

so the first iterate is given as

$$
\begin{aligned}
G^{[1]}(\vec{R}_{obs}|\vec{R}_{sp}) &= G_0(\vec{R}_{obs}|\vec{R}_{sp}) \\
&+ \int_{S_{UPPER}} [\nabla_{R_{fl}} G_0(\vec{R}_{UPPER}|\vec{R}_{sp}) G_0(\vec{R}_{obs}|\vec{R}_{UPPER})] \cdot \vec{n}_{UPPER} dS \\
&= G_0(\vec{R}_{obs}|\vec{R}_{sp}) \\
&+ \frac{1}{2} \int_{S_{UPPER}} [\nabla_{R_{fl}} G_0(\vec{R}_{UPPER}|\vec{R}_{sp}) G(\vec{R}_{obs}|\vec{R}_{UPPER})] \cdot \vec{n}_{UPPER} dS \\
&= G_0(\vec{R}_{obs}|\vec{R}_{sp}) - \frac{1}{2} G_0(\vec{R}_{obs\ upper\ image}|\vec{R}_{sp}) \ .
\end{aligned}
$$

The second iterate is given by

$$
\begin{aligned}
G^{[2]}(\vec{R}_{obs}|\vec{R}_{sp}) &= G_0(\vec{R}_{obs}|\vec{R}_{sp}) \\
&+ \int_{S_{UPPER}} [\nabla_{R_{fl}} G_0(\vec{R}_{UPPER}|\vec{R}_{sp}) G^{[1]}(\vec{R}_{obs}|\vec{R}_{UPPER})] \cdot \vec{n}_{UPPER} dS \\
&= G_0(\vec{R}_{obs}|\vec{R}_{sp}) \\
&+ \int_{S_{UPPER}} [\nabla_{R_{fl}} G_0(\vec{R}_{UPPER}|\vec{R}_{sp}) G_0(\vec{R}_{obs}|\vec{R}_{sp}) - \frac{1}{2} G_0(\vec{R}_{obs\ upper\ image}|\vec{R}_{sp})] \cdot \vec{n}_{UPPER} dS \\
&= G_0(\vec{R}_{obs}|\vec{R}_{sp}) - \frac{1}{2} G_0(\vec{R}_{obs\ upper\ image}|\vec{R}_{sp}) - \frac{1}{4} G_0(\vec{R}_{obs\ upper\ image}|\vec{R}_{sp}) \ .
\end{aligned}
$$

The n-th iterate has the simple form

$$
G^{[n]}(\vec{R}_{obs}|\vec{R}_{sp}) = G_0(\vec{R}_{obs}|\vec{R}_{sp}) - \left\{ \sum_{j=1}^{n} \frac{1}{2^j} \right\} G_0(\vec{R}_{obs\ upper\ image}|\vec{R}_{sp}) \ ,
$$

or

$$
G^{[n]}(\vec{R}_{obs}|\vec{R}_{sp}) = G_0(\vec{R}_{obs}|\vec{R}_{sp}) - \left\{ \sum_{j=1}^{n} \frac{1}{2^j} \right\} G_0(\vec{R}_{obs}|\vec{R}_{sp\ upper\ image}) \ .
$$

This final equation ends the supporting analysis for the main body of the report.

REFERENCES

McDaid, E. P., D. Gillette, and D. Baruch. 1992. *The Scattering of Sound from a Target in a Non-uniform Environment*. TR 1519 (Sep). Naval Command, Control and Ocean Surveillance Center, RDT&E Div., San Diego, CA.

Milton Abramowitz and Irene A. Stegun. *Handbook of Mathematical Functions*. Dover Publications, Inc., New York, 1964.

REPORT DOCUMENTATION PAGE

Form Approved
OMB No. 0704-0188

1. AGENCY USE ONLY *(Leave blank)*	2. REPORT DATE	3. REPORT TYPE AND DATES COVERED
	September 1994	Final: September

4. TITLE AND SUBTITLE

INTERACTIONS OF A TARGET WITH ITS ACOUSTIC ENVIRONMENT

5. FUNDING NUMBERS

AN: DN 302019
PE: 0602314N
PN: RJ14B28

6. AUTHOR(S)

E. P. McDaid, D. Gillette, and D. Barach

7. PERFORMING ORGANIZATION NAME(S) AND ADDRESS(ES)

Naval Command, Control and Ocean Surveillance Center (NCCOSC)
RDT&E Division
San Diego, CA 92152−5001

8. PERFORMING ORGANIZATION REPORT NUMBER

TR 1679

9. SPONSORING/MONITORING AGENCY NAME(S) AND ADDRESS(ES)

Office of Naval Research
Washington, DC

10. SPONSORING/MONITORING AGENCY REPORT NUMBER

11. SUPPLEMENTARY NOTES

12a. DISTRIBUTION/AVAILABILITY STATEMENT

Approved for public release; distribution is unlimited.

12b. DISTRIBUTION CODE

13. ABSTRACT *(Maximum 200 words)*

The results of a project to develop the capability to numerically model the sound scattered from a target in a dispersive environment are reported. The target has been rigorously coupled to its environment by combining a finite element formulation of the target shell dynamics with a Helmholtz Integral Equation formulation of fluid loading and a normal mode formulation of sound propagation. Though the computational cost of obtaining numerical solutions to this problem are awesome, some simple approximations can result in significant savings. In particular, neglect of Fresnel diffraction and boundary-induced multiple scattering permits a particularly simple and tractable reformulation of the problem.

The reported work makes the following contribution to solving the problem of target-environment interactions: the errors caused by neglecting Fresnel diffraction terms and multiple scattering are numerically evaluated. The significance of this contribution is that it will provide guidance as to when these useful approximations can be applied to speed calculations while still maintaining satisfactory fidelity. Also, additional numerical confirmation has been obtained of the significant violations of the sonar equation that can occur in dispersive environments. While the developed methodology is applicable to elastic targets, all calculated results detailed in this report are for cases of rigid targets. The inclusion of elasticity in this instance would not help to elucidate the phenomena of principal interest.

14. SUBJECT TERMS

acoustic
active sonar
antisubmarine warfare

15. NUMBER OF PAGES

16. PRICE CODE

17. SECURITY CLASSIFICATION OF REPORT	18. SECURITY CLASSIFICATION OF THIS PAGE	19. SECURITY CLASSIFICATION OF ABSTRACT	20. LIMITATION OF ABSTRACT
UNCLASSIFIED	UNCLASSIFIED	UNCLASSIFIED	SAME AS REPORT